ESTIMATION OF OIL CONSUMPTION DUE TO IN-CYLINDER VAPORIZATION IN INTERNAL COMBUSTION ENGINES

By

WILLIAM E. AUDETTE III

B.S., Mechanical Engineering (1997)
Bucknell University, Lewisburg, PA, USA

Submitted to the Department of Mechanical Engineering in
Partial Fulfillment of the Requirements for the Degree of
Master of Science in Mechanical Engineering

at the

Massachusetts Institute of Technology

June 1999

Signature of Author.....
Department of Mechanical Engineering
May 18, 1999

Certified By.....
Victor Wong
Lecturer, Department of Mechanical Engineering
Thesis Supervisor

Accepted By.....
Ain A. Sonin
Chairman, Department Committee on Graduate Students

ESTIMATION OF OIL CONSUMPTION DUE TO IN-CYLINDER VAPORIZATION IN INTERNAL COMBUSTION ENGINES

By

WILLIAM E. AUDETTE III

Submitted to the Department of Mechanical Engineering on May 18, 1999 in partial fulfillment of the requirements for the Degree of Master of Science in Mechanical Engineering

ABSTRACT

Two models were developed to estimate the rate of oil consumption due to the vaporization of oil from (1) the cylinder liner and from (2) the piston ringpack in an internal combustion engine. The purpose of the models is to gauge the importance of oil vaporization as a contributor to overall engine oil consumption. Another purpose of the models is to study the effect of various engine designs and operating conditions on oil vaporization.

The models are based on a mass convection analysis. Various sub-models for the establishing the state and properties of the engine oil as well as the convecting gas are presented. The model was implemented numerically and results were generated by simulating the behavior of a heavy-duty diesel engine.

Running at 2200 RPM and full load while using an SAE 15W40 oil, oil vaporization from the liner is seen to be about 1.3 grams per hour per cylinder, or about 10% of the total oil consumption for this engine. At the same conditions, oil consumption due to vaporization from the ringpack is found to be about 3.6 grams per hour per cylinder, or about 30% of the total oil consumption for this engine. Therefore, vaporization from in-cylinder sources appears to be a significant contributor to overall engine oil consumption.

For both models, the results are highly dependent upon the local temperatures and the local oil composition. Also, the high rates of vaporization seen from the ringpack may contradict the fundamental assumptions upon which the ringpack vaporization model was built. A study of liquid oil transport in the ringpack is required to fix this potential problem.

Thesis Supervisor: Victor Wong

Title: Manager, Sloan Automotive Laboratory

TABLES AND LISTS

1. TABLE OF CONTENTS

2. TABLE OF FIGURES

3. TABLE OF TABLES

INTRODUCTION

1. BACKGROUND

In light of tightening governmental regulations, controlling engine emissions is an important concern in engine design. While controlling the combustion of the fuel has perhaps the greatest impact on emissions, the influence of the lubricating oil has been receiving attention as well.

The physical mechanisms through which the lubricating oil influences engine emissions are not clear though it has been suggested that the vaporization of oil from the cylinder liner may be a contributor [1][2]. Also, it is hypothesized here that oil is also being vaporized by the gas flow around the piston and its crevices. Oil vaporized from any of these exposed surfaces within the engine is presumed to join the cylinder gases and leave the engine as either partially burned or unburned hydrocarbons. Reducing oil consumed through vaporization should reduce hydrocarbons in the exhaust and, therefore, should help to reduce overall engine emissions.

Currently, research is being aimed at discovering which design parameters and lubricating oil properties most greatly affect the vaporization of oil from an internal combustion engine (ICE). Here at MIT, it has been decided to create physically based computer models of the piston-ringpack-liner system so that the behavior of the system can be studied.

2. PISTON-RINGPACK-LINER MODELING AT MIT

The behavior of the piston-ringpack-liner system is very dynamic. The interactions between the piston, rings, and cylinder liner are complex. Their motions are dependent on a number of factors – none of which are well understood. For example, the dynamics of the rings alone are a function of the gas flow through the ringpack, the geometry of the rings and groove, and the friction (and, therefore, the oil lubrication state) between the ring face and the liner. This high amount of coupling between the various bodies, the lubricating oil, and the gas flows means that modeling the system will not be easy.

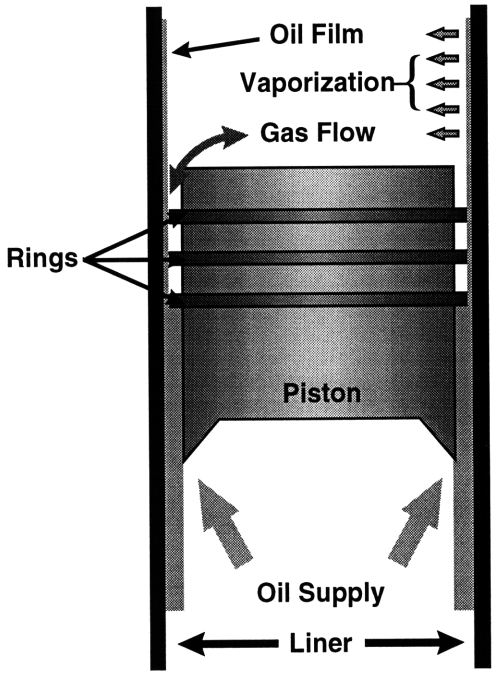

Figure 1: Depiction of piston-ring-liner system

At MIT, the approach to solving this problem has been to separate the analysis of the governing motions of the system from the oil consumption analysis. In this context, knowledge of the governing motions includes knowing the position/velocity/acceleration of each body in the system as well as knowing the time history of gas flows and liquid oil distribution within the system. Making the analysis of the governing motions separate is useful because it appears that the coupling of oil consumption to governing motions is mostly one-directional – oil consumption is highly dependent on the governing motions but the governing motions are not highly dependent on the gas flows. This hypothesis will have to be checked once results are generated.

To generate the governing motion data of a piston-ringpack-liner system, the Sloan Automotive Laboratory at MIT has created several physics-based computer models. The models relevant to the estimation oil vaporization are described below:

Ringpack-OC: The Ringpack-OC model is used to compute the motion of the piston rings within their grooves. Driving this system are inertial forces (due to axial piston motion), ring-liner friction, and gas flows. Since the gas flows between the combustion chamber, ringpack crevices, and crank-case are not known *a priori*, they are computed here. More information can be found in [3].

Friction-OFT: The Friction-OFT model is used to compute the friction force resulting from the piston rings sliding along the cylinder liner. The model predicts

the oil film thickness (OFT) along the cylinder liner resulting from the motion of the piston rings. Also, instantaneous ring wetting data such as OFT under each ring, oil attachment points on the face each ring, and oil scraped by each ring are all generated by this model. More information can be found in [4].

As input, both of these models require detailed knowledge of the geometry of the system, the viscosity properties of the lubricating oil, and a pressure trace of the gas in the combustion chamber through one 720 degree 4-stroke cycle. The models were created as both an analysis tool to help understand experimental data and as a predictive tool to help find desired behavior when designing the system.

In developing oil vaporization models, the Ringpack-OC and Friction-OFT models will be used to describe the instantaneous governing motions of the system. Much of this data is difficult or impossible to obtain experimentally. Also, these computer tools are much more convenient for running parametric studies (answering "what if..." questions) as compared to trying to locate or generate experimental data.

3. PURPOSE OF VAPORIZATION MODELS

Building on the approach used by the Friction-OFT and Ringpack-OC models, new models have been created to estimate the amount of oil vaporized from the cylinder liner and from the piston-ringpack surfaces. The purpose of these models is to gauge the relative importance of oil vaporization to the overall oil consumption of the engine. In addition, the models can be used to evaluate the influence of various engine design parameters and oil properties on the rate of oil vaporization.

In the end, the models should establish if oil vaporization is an important source of oil consumption and they should show how the vaporization could be reduced.

4. MODELING PLAN

For the vaporization models, the same approach has been taken as for the other MIT piston-ringpack-liner models. The vaporization models contain the physics believed to be relevant to oil vaporization. The models are then implemented numerically in the form of a computer program. Detailed geometry and operating conditions can be included as input, though the level of detail

needed was tempered by the desire to keep the models simple enough so that they could be easily used while still providing meaningful results.

The models operate on a crank-angle by crank-angle basis and can provide detailed information as to what the model believes to be the internal state of the system. In the course of developing the models, the end results as well as the internal states of the system were checked against intuition and against industrial experience. If anything seemed inappropriate or difficult to believe, additional physics would be added (or removed) to try and capture the experimentally observed behavior of the system.

As with any modeling initiative, the models can be forever improved and expanded. The state of the models as presented in this report do not necessarily represent what is believed to be the best models achievable. Rather, they are presented as the models achieved given the prior 2 years of work. Certainly, improvements can be made in some areas. Those improvements are left for other studies at a later date

5. DOCUMENT STRUCTURE

This report will document the models created and the results generated during the examination of oil vaporization at the Sloan Automotive Laboratory at MIT over the past 2 years. Two models were created to specifically look at oil vaporization. The two models are discussed separately in this report.

Chapter 2 discusses the model that was used to estimate the rate of oil vaporization from the cylinder liner. Much of this text (absent the additions and edits present in this version) can be found in a technical paper published by the Society of Automotive Engineers International as paper number 1999-01-1520.

Chapter 3 is an extension of the work presented in Chapter 2. Here, the liner oil vaporization model is coupled to the liner oil film thickness model, Friction-OFT. Using the coupled model, oil transport rates along the cylinder liner are explored. Cases were run to attempt to alter these transport rates. The resulting effects on oil vaporization from the liner are shown.

Chapter 4 presents the model developed to estimate the rate of oil consumption due to vaporization from the surfaces of the ringpack. While the model seemed to function properly, the results challenge the basic assumptions upon which the model was built. The development and

inclusion of a liquid-oil transport model for the ringpack is an excellent next step to improve the ringpack oil vaporization model.

In each of these three chapters, the physics included in each model are defined, the numerical implementation is discussed, and results are presented.

Chapter 5 summarizes the current state of oil vaporization modeling and discusses future work that can be done based on the work presented here.

ESTIMATING OIL VAPORIZATION FROM THE CYLINDER LINER

ABSTRACT

A model has been developed for estimating the oil vaporization rate from the cylinder liner of a reciprocating engine. The model uses input from an external cycle simulator and an external liner oil film thickness model. It allows for the change in oil composition and the change in oil film thickness due to vaporization. It also estimates how the passage of the compression and scraper rings combine with the vaporization to influence the steady-state composition of the oil layer in the upper ring pack.

Computer model results are presented for a heavy-duty diesel engine using a range of liner temperatures, several engine speeds, and two different oils. Vaporization from the liner at 2200 RPM and full load is found to be about 1.1 grams per hour per cylinder. This represents about 10% of the total oil consumption for this engine. Vaporization is found to be highly dependent on liner temperature and steady-state oil composition. Little dependence on engine speed is seen. The steady-state oil composition near the top of the cylinder is found to be significantly different than the composition of the oil near the bottom of the cylinder.

1. INTRODUCTION

In light of tightening governmental regulations, controlling engine emissions is an important parameter in engine design. While the combustion of the fuel has perhaps the greatest impact on emissions, the influence of the lubricating oil has been receiving attention as well.

The physical mechanisms through which the lubricating oil influences engine emissions still are not clear though it has been suggested that the vaporization of oil from the cylinder liner may be a contributor. Oil vaporized from exposed surfaces within the engine is presumed to join the cylinder gases and leave the engine as either partially burned or unburned hydrocarbons. Reducing oil

consumed through vaporization should reduce hydrocarbons in the exhaust and, therefore, should help to reduce overall engine emissions.

A study by Orrin and Coles [1] suggests that the vaporization of oil from the liner has a significant influence on the overall oil consumption. For two identical grades of oil, for example, they found that the oil with a higher fraction of volatile compounds had much higher rate of oil consumption.

A study by Furuhama et al. [2] found similar results and also added that oil consumption was seen to be more strongly dependent on liner temperature when the more volatile oils were used.

Several models for the vaporization of oil from the cylinder liner have been presented in an attempt to establish which physical mechanisms and which design parameters most strongly influence oil vaporization. One of the most complete models presented thus far is by Wahiduzzaman et al. [3]. At its core, their model treats oil vaporization as the diffusion of oil vapor through a gas boundary layer on the cylinder's surface. The oil itself is modeled as being composed of several distinct hydrocarbon species each with its own boiling point and associated vapor pressure. Overall oil vaporization is computed by computing the local instantaneous oil vapor mass flux for numerous locations on the liner, integrating over time and space, and summing over the number of oil species.

For the heavy-duty diesel engine that they modeled, their results show that oil vaporization is a small contributor to overall oil consumption (2-5%). They found that oil consumption was sensitive to oil grade and cylinder temperature. Interestingly, their model also showed that under certain conditions most of the oil vaporization occurs during the non-firing half of the engine cycle.

All of these trends were confirmed with a less complex (single species oil) model presented by Petris et al. [4].

With these results in mind, it was decided to extend many of the ideas used in the Wahiduzzaman model [3] and to create the model presented here. Specifically, the modeling of the oil properties will be more robust here.

It was decided, for example, to allow all the oil properties to vary from species to species (not just boiling point and vapor pressure). Also, it was decided to allow the default composition of the oil to vary from location to location along the liner. The previously published models seem to require that the initial oil composition be the same for all points on the liner. It does not seem reasonable to assume that composition of the oil in the cool lower region of the liner should necessarily be the same

as the hot upper region of the liner which the oil control ring cannot reach. This restriction was removed from our model. Extending this idea, our model will also compute the steady-state oil composition automatically. Only the default composition of the oil being supplied to the liner need be specified.

2. MODEL DESCRIPTION

In the current model, oil vaporization is treated as a mass convection problem -- oil vapor at the surface of the liquid oil film is carried away by the motion of the cylinder gases. The oil is modeled as being composed of several discrete hydrocarbon species each with its own thermo-physical properties. The average rate of oil vaporization, therefore, is computed by calculating the local instantaneous mass flux for each oil species for several locations (distributed axially) along the liner, summing those fluxes over the number of species, integrating over the surface of the liner, and averaging over one engine cycle. Stated in a more compact form, the time averaged oil vaporization rate, M, is found by

$$M = \frac{2\pi R}{T} \int\int \sum_i m_{e,i}(x,t)\, dx\, dt \tag{1}$$

where R is the cylinder radius, T is the period of one cycle, and $m_{e,i}$ is the local instantaneous evaporative mass flux for a given oil species i.

To evaluate the integral in x, the surface of the cylinder liner is divided axially into a number of discrete points (figure 2). A local evaporative mass flux is computed at each location based on the local temperature, local oil properties, local oil vapor properties, and overall cylinder gas properties. The space integral in equation (1) is then computed numerically for the portion of the liner that is above the piston top and, therefore, exposed to the cylinder gases.

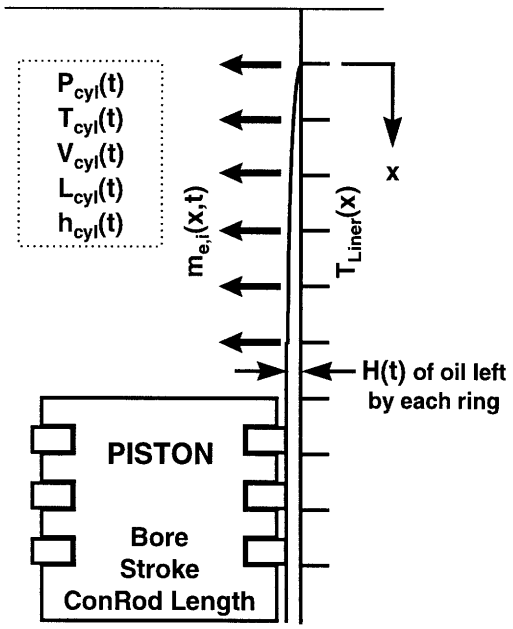

Figure 2: Piston-ring-system and some parameters affecting oil vaporization

2.1. Convection Model

To evaluate the local instantaneous evaporative mass flux, the standard model for convective mass transport [5] is used such that

$$m''_{e,i}(x,t) = g_{m,i}(x,t) \cdot \left(mf_{s,i}(x,t) - mf_{\infty}\right) \tag{2}$$

where $g_{m,i}$ is the mass convection coefficient for a particular oil specie, $mf_{s,i}$ is the mass fraction of oil vapor at the cylinder surface for that specie, and mf_{∞} is the mass fraction of that species in the bulk cylinder gasses. Due to the large mass of cylinder gasses relative to the small mass of expected oil vapor, mf_{∞} is assumed to be zero. The vapor mass fraction at the oil film surface is computed from the local vapor pressure of the oil species of interest.

2.2. Oil Model

To account for the complex volatility behavior of engine oils, the oil is modeled as being composed of several pure hydrocarbon species. The boiling point and mass fraction (relative to the liquid oil) for each species must be specified. This data can be taken from a distillation curve (Fig 3) for the oil of interest.

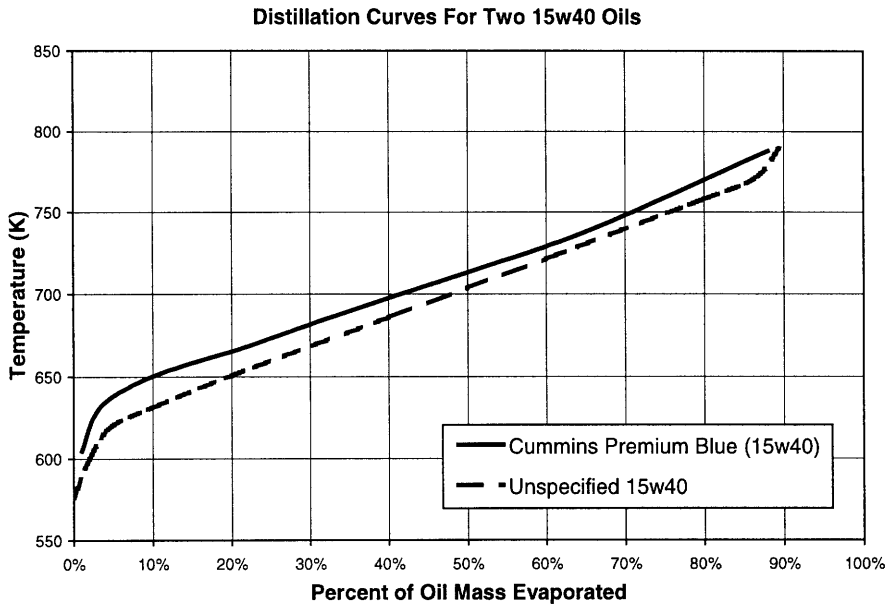

Figure 3: Distillation curves for two 15W40 oils used in this study

Once the boiling point and mass fraction for an oil species is specified from the distillation curve, all the other necessary oil vapor properties for that species can be computed (see Appendix A for details on property calculations). For equation (2), the mass fraction of each oil species is calculated as

$$mf_{s,i}(x,t) = \left(\frac{\overline{mf_{l,i}(x,t)} \cdot P_{v,i}(T_s)}{P_{cyl}(t)} \right) \left(\frac{MW_i}{MW_\infty} \right) \tag{3}$$

with $\overline{mf_{l,i}}$ as the local instantaneous *mole fraction* of the species in the liquid oil film, $P_{v,i}(T_s)$ is the vapor pressure of the oil species at the local instantaneous temperature of the surface of the oil film, $P_{cyl}(t)$ is the instantaneous pressure of the bulk cylinder gas, MW_i is the molecular weight of the oil specie, and MW_∞ is the average molecular weight of the gas in the wall boundary layer. Since the total molar fraction of the oil species in the boundary layer gas is low, MW_∞ is taken to be the molecular weight of air.

2.3. Evaluating Convection Coefficients

With mf_∞ and $mf_{s,i}$ specified, only the mass convection coefficient g_m in equation (2) remains to be evaluated. The mass convection coefficient is computed in this model using the analogy between heat and mass transfer. In such analyses, a heat convection coefficient, h, is computed from a Nusselt-Reynolds-Prandtl correlation [5] such as

$$Nu = a \cdot \mathrm{Re}^{d} \cdot \mathrm{Pr}^{e} \tag{4}$$

where

$Nu = \mathrm{hL/k}$: Nusselt Number
$\mathrm{Re} = \mathrm{VL}/\upsilon$: Reynolds Number
$\mathrm{Pr} = \upsilon/\alpha$: Prandtl Number

L : Characteristic Length
V : Characteristic Velocity
k : Thermal Conductivity
υ : Kinematic Viscosity
α : Thermal Diffusivity

Using the analogy between heat and mass transfer, the corresponding mass transfer relation is

$$Sh = a \cdot \mathrm{Re}^{d} \cdot Sc^{e} \tag{5}$$

where

$Sh = (g_{m}\mathrm{L})/(\rho \mathrm{D}_{ab})$: Sherwood Number
$\mathrm{Re} = \mathrm{VL}/\upsilon$: Reynolds Number
$\mathrm{Sc} = \upsilon/\mathrm{D}_{ab}$: Schmidt Number

ρ : Density
D_{ab} : Binary Diffusion Coefficient

Of course, for this analogy between heat and mass transfer to remain valid, the rate of oil vaporization must remain low enough for the process to be considered a low mass transfer rate convection process. Also, the temperature of oil film must not exceed the boiling point for any of the oil species for the given cylinder pressure. Boiling is an energy limited process and equation (2) only applies for diffusion limited process.

Many attempts have been reported to determine appropriate values for the constants *a, d,* and *e* in equations (4) and (5). Several studies (summarized in [6]) were conducted which tried to fit experimental results to equation (4). Suggested values are

$a = 0.035$ to 0.13
$d = 0.7$ to 0.8
$e = 0.667$

2.4. Evaluating Fluid Properties

To calculate g_m from the Sherwood-Reynolds-Schmidt relation (equation (5)), it is necessary to know many of the cylinder gas properties. The properties of the bulk cylinder gas, such as the cylinder gas temperature, pressure, velocity, and characteristic length of motion, must all be taken from an external cycle simulation model. The binary diffusion coefficient is computed for each oil species using a temperature and pressure dependent procedure summarized by Lyman, Reehl, and Rosenblatt [7]. All properties for air are taken from standard air tables (indexed by temperature and corrected for pressure) while all oil vapor properties are computed as seen in Appendix A. All temperature dependent properties are evaluated at the average between the local instantaneous liner oil temperature and the bulk cylinder gas temperature.

While the temperature of the bulk cylinder gas is given by the external cycle simulator, the temperature of the oil film must be calculated. This temperature can be computed by knowing the local cylinder liner temperature and by knowing the heat flux from the cylinder gas to the cylinder liner. The heat flux must be given by the cycle simulator either directly or in the form of heat convection and radiation heat transfer coefficients. When the heat flux is known, then the temperature of the surface of the oil film, T_s, can be estimated by assuming quasi-steady-state, one-dimensional heat conduction through the oil film

$$q''_{conv}(x,t)+q''_{rad}(x,t)-q''_{vap}\left(\sum_i m_{e,i}(x,t)\right)=k\frac{T_s(x,t)-T_{liner}(x)}{H(x,t)} \tag{6}$$

where q''_{conv} is the heat flux into the oil due to convection from the cylinder gas, q''_{rad} is the heat flux into the oil due to radiation from the cylinder gas, q''_{vap} is the latent heat required to vaporize the amount of oil specified by the total evaporative mass flux at that location ($\sum_i m_{e,i}$), k is the thermal conductivity of the liquid oil, T_{liner} is the specified local temperature of the cylinder liner, and H is the current thickness of the oil film at the location in question. The liner temperature, T_{liner}, is assumed to be a function of the temperature at top-dead-center, T_{TDC}, and the temperature at bottom-dead-center, T_{BDC}, following the trend suggested by [8]

$$T_{liner}=T_{TDC}-(T_{TDC}-T_{BDC})\sqrt{\frac{x}{Stroke}} \tag{7}$$

Due to the interdependence of mass flux and oil film surface temperature in equations (2) through (6), the solution for the mass flux must be solved iteratively.

2.5. Integration and Initial Conditions

With the local instantaneous mass flux solved, the instantaneous oil vaporization rate is found by carrying out the space integral in equation (1). The average vaporization rate is then found by evaluating the time integral. Of course, to do this time integral, initial conditions must be specified. In this model, the desired output is the data dealing with the mass evaporated. The variables that must be tracked through time, though, are the masses of each species available at each location on the liner. The initial conditions, therefore, describe the amount of each oil species at the each location at the beginning of an engine cycle.

Using the notation in the previous equations, the initial conditions could be specified by giving the initial oil film thickness at all locations, $H(x,0)$, the density of the liquid oil, ρ_l, and the initial mass fraction of each species at each location in the oil film, $mf_{l,i}$. Taken together, they specify the mass of each oil species available. Once these quantities are specified, they are free to change through time. The oil film thickness, for example, will shrink as oil is vaporized and as the rings pass by. The species mass fractions will also change as the more volatile species vaporize away more quickly than the heavier ones.

The simplest way to specify the initial values would be to assume that both the oil film thickness and the oil composition is the same everywhere on the liner. This, however, is not a realistic condition knowing that oil film thickness depends on the motion of the piston and the performance of the piston rings. Also, it should be expected that the steady-state oil composition in the hot upper region of the cylinder liner is different than the oil in the cooler lower part.

To provide more realistic initial conditions, the results from an external ring-pack dynamics and liner lubrication model can be used. For this study, a computer models by Tian et al. [9] is used which predicts the thickness of the oil film left on the liner by the passage of each ring in the three-ring system. This model accounts for Reynolds, boundary, and mixed lubrication regimes as well as complex piston, ring, ring face, and ring groove geometry and the associated ring motion [10]. The model directly provides liner oil film thickness at the end of the intake and expansion strokes. These film thickness profiles are used in the vaporization model presented here as $H(x,0)$. The lubrication model, though, also gives the instantaneous wetting condition of each ring as well as the before and after oil film thickness for each ring on a crank-angle by crank-angle basis. Combined with the local instantaneous vaporization rate, this additional information also allows $H(x,t)$ to be calculated as the vaporization model integrates through time.

2.6. Choosing Initial Oil Composition

Deciding upon an appropriate initial composition for the liner oil is not as easy as the calculation for the oil film thickness described above. The easiest approach may be to view the liner as having two regions – one region that is passed by the oil control ring and a second region above the top-dead-center of the oil control ring (figure 4).

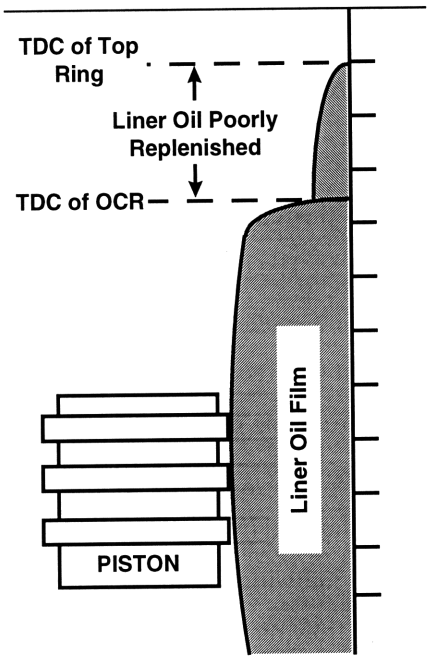

Figure 4: Composition of oil film near TDC may be very different due to poor replenishment by piston rings

For the lower region (the region affected by the oil control ring), it is assumed that the quantity of oil circulating through the oil control ring and piston skirt is high enough to completely refresh the oil left on the liner. The oil composition in the region, therefore, can be assumed to be the same as the oil circulating through the rest of the engine (as given by a distillation curve).

For the upper region of the liner where the oil control ring does not reach, however, it is more difficult to know the composition of the oil film *a priori*. Since this oil is not refreshed by the oil control ring, the only factors influencing its composition are the loss of volatile compounds due to vaporization and the passage of the compression and scraper rings. Compared to the oil control ring, the top two rings are much more oil starved and will not carry much fresh oil to the upper part of the cylinder liner. The oil in the upper part of the liner, therefore, will most likely be depleted of its more volatile species.

To model this effect, it is assumed that the oil carried along with the face of the ring is the only supply of oil to the upper part of the cylinder liner. As a ring passes a point on the liner, the

composition of the oil film at that location will probably change to reflect the intermingling with any oil that has been brought up from the lower region of the liner. The change in composition due to the passage of each ring must be calculated. If this change in composition can be modeled and coupled to the vaporization model, then the overall model can be run over and over until a steady-state composition is found for the oil film. The steady-state composition will reflect the oil inflow brought by the rings balancing the oil outflow experienced through vaporization.

2.7. Calculating Change in Oil Composition Due To Ring Passage

The calculation of the influence of ring passage on liner oil composition must begin with a statement of conservation of mass. In this case, a control volume is drawn around the ring and its surrounding oil film as shown in figure 5. The control volume is attached to the frame of reference of the ring (ignoring any ring rotation). The control volume is wide enough so that the height of the oil layer is not influenced by the approaching or receding rings. Since the control volume is in the frame of reference of the ring, oil is seen entering one side of the control volume and leaving the other. The heights of the inflow or outflow may be different depending on if the ring is moving away from or moving closer to the cylinder liner (as dictated by the lubrication conditions). The mass flow rate into the control volume can be computed by knowing the speed of the piston and the height of the oil layer entering the control volume. The mass flow rate out of the control volume is computed similarly.

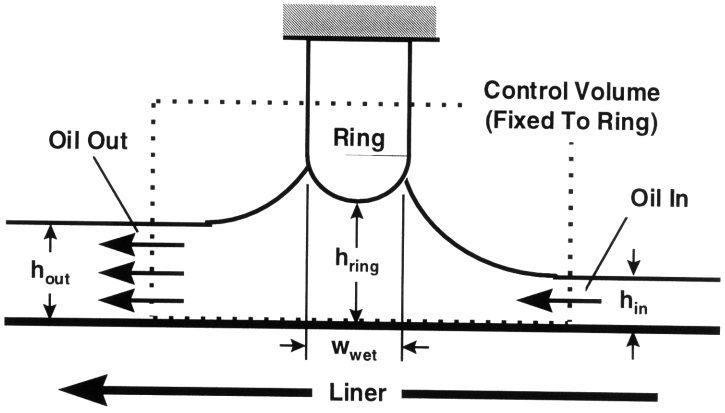

Figure 5: Control volume fixed to ring and the oil flows as seen in the frame of reference of the ring.

Normally, a conservation of mass equation would now be applied to track the amount of mass of each oil species that enters, leaves, and accumulates in the control volume. In this situation, though, the external ring-dynamics/oil-film-thickness model generates nearly all the relevant data. The model gives as output the heights of the oil layer as well as the wetting width for each ring. Therefore, the overall volume of oil in the control volume is known for all time. It is not necessary to

perform the complete mass conservation on the control volume because the external ring-dynamics/oil-film-thickness model has done it already [9,10].

It is necessary, however, to track the composition of the oil entering, leaving, and being stored in the control volume attached to each ring. To do this, it is still necessary to apply a conservation of mass to the control volume attached to the ring. The difference, though, is that instead of explicitly keeping track of the *mass* of each species, the *mass fraction* of each species is tracked. By tracking the mass fraction, the computations are more numerically stable since the results are, by definition, already non-dimensional and normalized.

When applying a conservation of mass to the multi-species oil, one conservation of mass equation will results from every species composing the oil. The conservation of mass equation for each species *i* can be written as (see Appendix B for derivation)

$$\frac{d}{dt}\left(mf_{stored,i} \cdot Vol\right) = Vel \cdot 2\pi \cdot R \cdot \left(\left(h_{in} \cdot mf_{in,i}\right) - \left(h_{out} \cdot mf_{out,i}\right)\right) \tag{8}$$

where the subscript *stored* refers to the amount of that quantity within the control volume, *mf* is the mass fraction of the specie, *Vol* is the instantaneous volume of oil within the control volume, *Vel* is the instantaneous velocity of the oil entering/leaving the control volume (e.g. the piston velocity), *R* is the radius of the cylinder, and *h* is the height of the oil layer at the location specified. Note that the volume and all the heights can be computed directly from the output of the ring-dynamics/liner-oil-film model. Also, the $mf_{in,i}$ is known from the initial conditions or previous calculations in the vaporization model. To solve for the rate of change of $mf_{stored,i}$, therefore it is necessary to know the composition of the oil leaving the control volume, $mf_{out,i}$.

The normal assumption in such control volume analyses that the species within the control volume are well-mixed. In well-mixed situations, the oil stored in the control volume mixes with the oil entering the control volume. Also, the composition of the mixture exiting the control volume has the same composition as the mixture stored in the control volume. For interaction between the ring and liner oil, though, the oil is so viscous that the oil flow is almost certainly laminar under the ring (speculation). Since laminar flows have little if any mixing, a better modeling assumption is that less mixing is occurring under the ring.

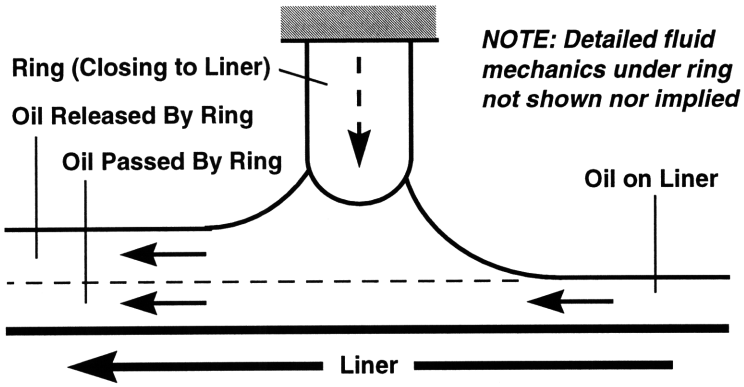

Figure 6: Entering oil passing through control volume

Figure 6 shows how such rules for computing the oil composition are visualized. The basic premise to the mixing rules used in this model is that any oil entering the control volume passes straight through the control volume if possible (as defined by the model by Tian *et al.* [9]). If more oil is entering than exiting, the oil exiting the control volume has the same composition as the entering oil because the exiting oil passed straight through without mixing with the oil accumulated under the ring. The excess oil entering the control volume does mix with the accumulated oil and this changes the oil composition based on the typical mass conservation relations for a control volume.

If, on the other hand, more oil is exiting the control volume than entering, the oil entering does pass through the control volume and becomes part of the oil exiting the control volume. The extra oil required to make up the rest of the exiting flow comes from the oil accumulated in the control volume. The total exiting flow is considered to be well-mixed whose composition is a weighted average of the incoming oil composition and the composition of the accumulated oil. The composition of the accumulated oil does not change in this case because none of the entering oil is being accumulated.

Speaking mathematically, the rules described above define the mass fraction of each species exiting the control volume as

$$\begin{aligned} &\text{If } h_{in} \geq h_{out} : \; mf_{out,i} = mf_{in,i} \\ &\text{If } h_{in} < h_{out} : \; mf_{out,i} = \frac{h_{in} \cdot mf_{in,i} + (h_{out} - h_{in}) \cdot mf_{stored,i}}{h_{out}} \end{aligned} \tag{9}$$

With equation (9), it is now possible to solve equation (8) and track through time the composition of the oil carried with the rings. Even more importantly, equation (9) states how the composition of the oil left on the liner changes by the passage of a ring. Referring back to the previous argument, the initial conditions can be found by applying some default composition (say that of fresh oil) and by letting the vaporization model run repeatedly until a steady-state liner oil

composition is found. The average vaporization rate, therefore, is the average vaporization rate using the newly-found steady-state oil composition (note: due to the complexities of modeling the oil control ring, it is assumed that the oil below the TDC of the oil control ring is completely refreshed to default oil composition with each passage of the rings).

3. RESULTS AND DISCUSSION

To generate the results presented in this section, a heavy-duty Cummins diesel engine was modeled. Some of the relevant engine design parameters are given in the table below.

Table 1: Basic geometry of the engine simulated here

Bore	114 mm
Stroke	135 mm
Compression Ratio	17.2:1

Several cases were run in order to examine the influence of several parameters on vaporization. Specifically, the effect of liner temperature, oil composition, and speed were all examined. Also, the model's sensitivity to the user-defined mass transfer parameters (equation (5)) was determined.

3.1. Description of Baseline Case

To properly gage the effect of each parameter of interest, baseline values were established from which each parameter could be varied. The baseline operating condition used in this study is shown in the table below

Table 2: Baseline operating condition and vaporization model parameters

Liner Temp – Top Dead Center	160 C
Liner Temp – Bottom Dead Center	112 C
Speed (RPM)	2200 RPM
Mass Transfer Parameter – a	0.035
Mass Transfer Parameter – d	0.8

Detailed geometry and operating conditions for this engine are used to run a cycle simulator, a ring and gas dynamics model, and a linear oil film thickness model. Some results from these models are presented in figures 7-10 for the baseline case

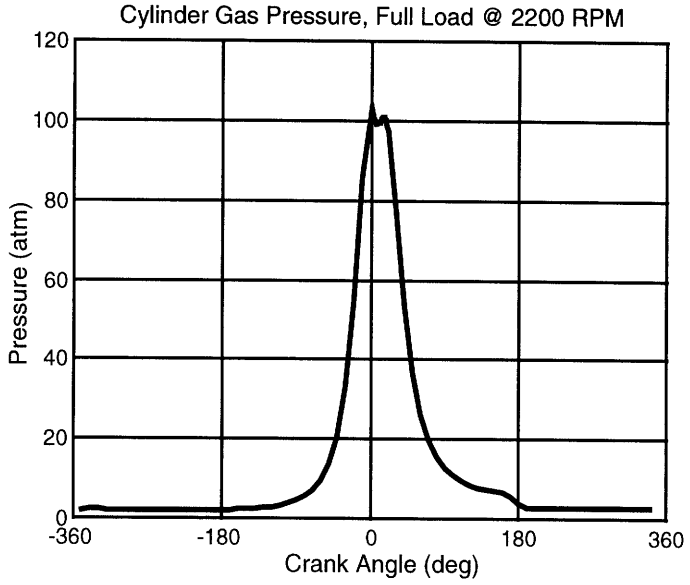

Figure 7: Estimated cyclic variation of the pressure of the cylinder gases at full load and 2200 RPM

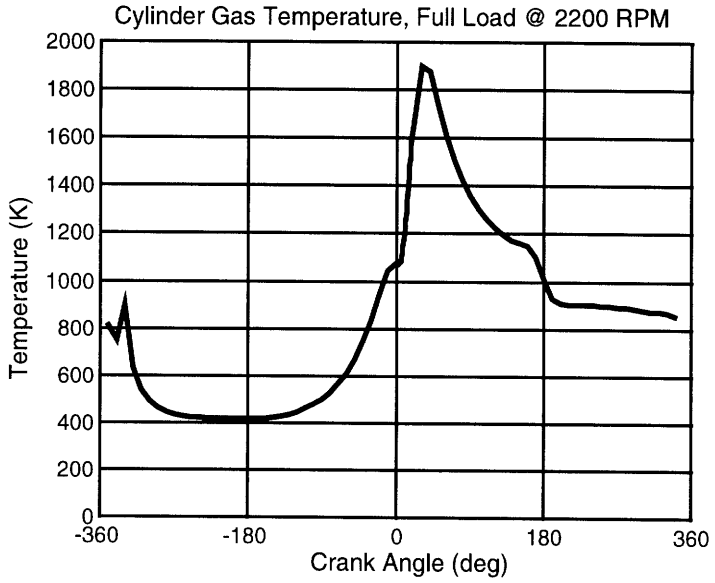

Figure 8: Estimated cyclic variation of the cylinder gas bulk temperature at full load and 2200 RPM

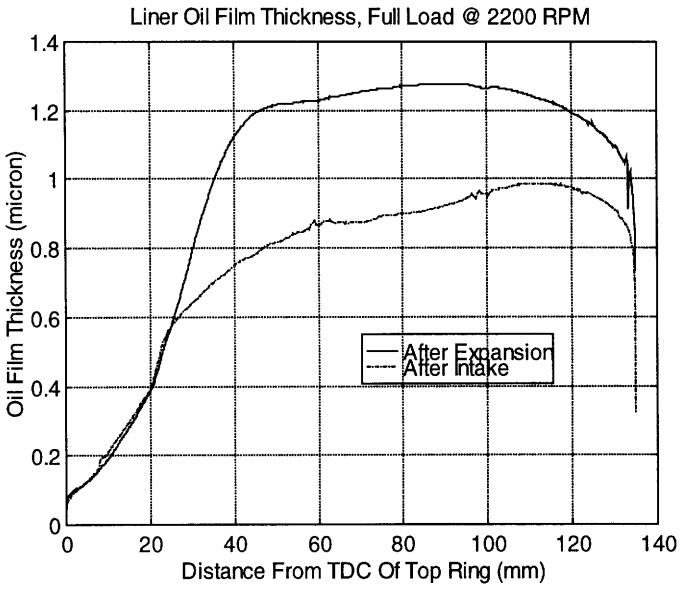

Figure 9: Estimated liner oil film thickness after intake and expansion strokes at full load and 2200 RPM

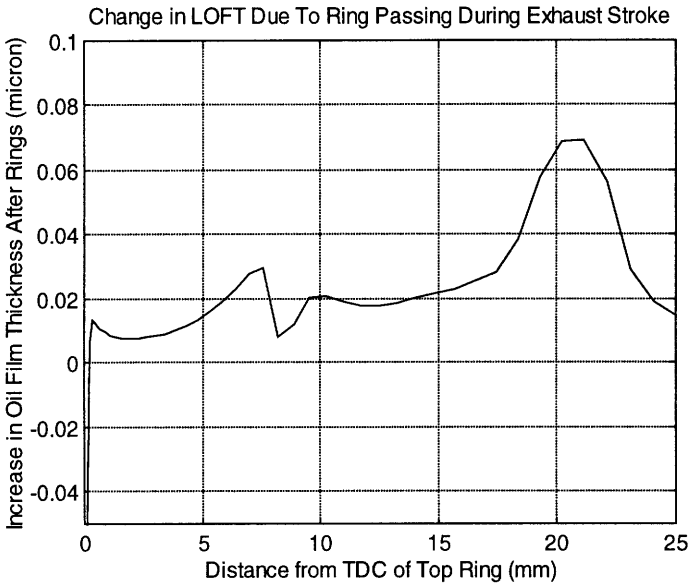

Figure 10: Estimated change in oil film thickness due to passage of rings during exhaust stroke at full load and 2200 RPM

In figure 9, notice that the liner oil film thickness is much thinner in the upper part of the liner (axial position less than 20 mm). This reflects the fact that the oil supply to upper region is much lower than the supply to the lower region of the cylinder liner. The oil supply is less because the oil control ring cannot reach the upper part of the liner. For this particular engine, the oil control ring is approximately 27 mm below the top ring. Any oil supplied to the liner within 27mm of TDC position of the top ring, therefore, must come from oil carried with the top two rings.

Figure 10 shows how the top two rings can carry oil to the upper portion of the ringpack (and can, therefore, affect its composition). This figure shows that the liner oil film in the upper portion of the liner is thicker after the exhaust stroke than it was before the exhaust stroke. The figure shows the combined effects of the top and second rings. Since there is a net increase in thickness by this stroke, oil must be being released from the rings. Oil, therefore, is being supplied to the upper part of the liner during the exhaust stroke.

3.2. Description of Engine Oils

With the data from the cycle simulation, ring dynamics, and liner oil film models, all that remains to be specified is the type of oil to be used. For this study, two oils were used – Cummins Premium Blue (SAE 15W40) and an unspecified 15W40 taken from the literature [3]. The distillation curve for each oil is presented in Figure 3. Even though both are SAE 15W40 class oils, notice that the Cummins Premium Blue has a significantly higher distillation curve. Both oils were modeled as being composed of 10 pure hydrocarbon species with more species used to model the highly-sloped lower region of the distillation curve.

3.3. Dependence of Vaporization on Liner Temperature

Figure 11 shows the oil vaporization rate at the baseline operating condition using the Cummins Premium Blue oil. To generate these values, it was assumed that the initial oil composition was that of the Premium Blue as defined by the distillation curve. The oil was discretized into 10 species and the cylinder liner was discretized axially into 30 nodes – ¾ of which were evenly spaced above the TDC of the OCR. By running the model repeatedly, the oil vaporization rate eventually reached a steady value. This iterative procedure allows the oil in the upper part of the liner to change its composition (i.e. become depleted of lighter species). With each iteration, the oil becomes heavier until the oil mass lost due to vaporization is balanced by the oil mass supplied by the piston rings. It is these steady-state, depleted-oil vaporization rates that are reported in Figure 11.

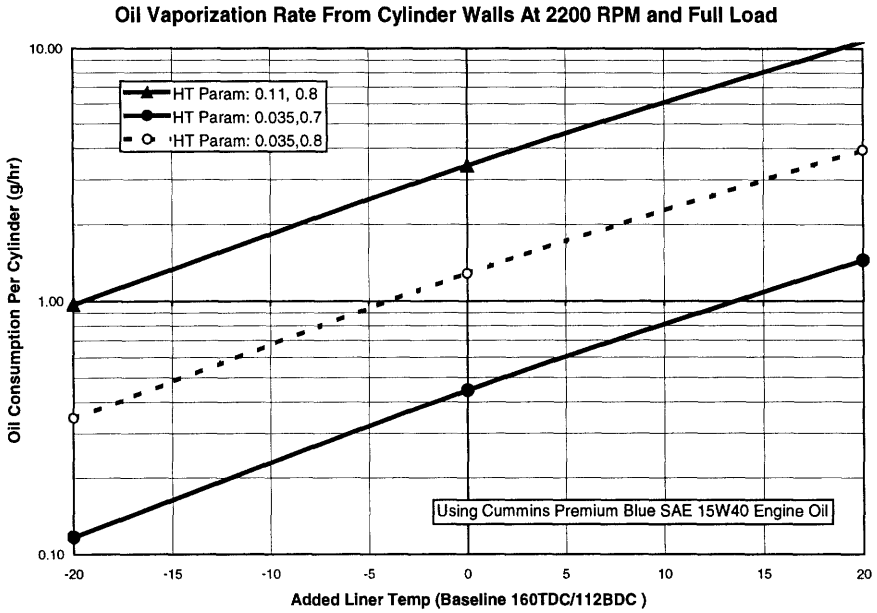

Figure 11: Average liner oil vaporization rate per cylinder at baseline conditions showing effect of varying the liner temperature and of varying the mass transfer parameters

In this figure, the vaporization rate at baseline conditions is 1.28 g/hr/cylinder (the point at the center of the figure). The overall oil consumption for this engine is expected to be 10-13 g/hr/cylinder. Oil vaporization from the cylinder liner appears to be the source for about 10% of the overall oil consumption.

Figure 11 also shows the sensitivity of vaporization to liner temperature. To the left and right of the baseline case, vaporization rates are reported using a liner temperature that is 20 degrees hotter or colder (20 degrees has been added or subtracted to both the TDC and BDC temperatures). As can be seen, the vaporization rate is strongly dependent on the liner temperature. On average, the vaporization increases an order of magnitude for every 38 degrees Celsius increase in the liner temperature.

Finally, figure 11 shows the dependence of the oil vaporization rate on the assumed values for the mass transfer (MT) parameters a and d used in equation (5). On average, the maximum values for the MT parameters produced a vaporization rate about 3 times that calculated at the baseline conditions. The minimum MT parameters yielded a rate 1/3 that at the baseline conditions.

3.4. Dependence of Vaporization on Oil Composition

To see the effect of allowing the model to find the steady-state, depleted-oil solution, figure 12 compares the vaporization rates using various models for the composition of the oil on the portion

of the liner above the top-dead-center of the oil control ring. In all cases, the oil on the liner below the TDC of the OCR is assumed to be fully replenished by the passage of the OCR. To avoid confusion when interpreting this graph, the solution presented as "Using Depleted Oil Above TDC of OCR" represent the same data points as those shown in figure 11 using the baseline mass transfer parameters (a=0.035, d=0.8) in equation (5).

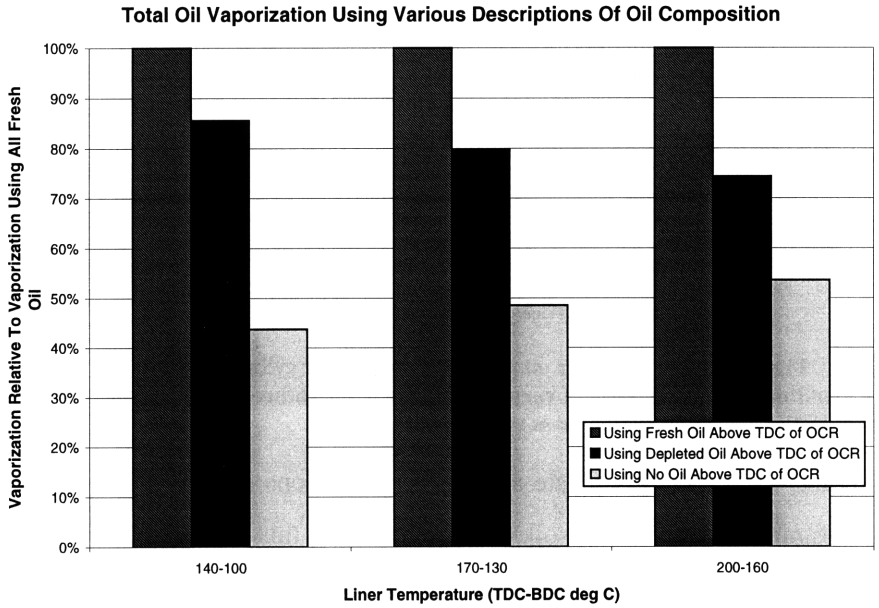

Figure 12: Total oil vaporization from liner at baseline conditions using (1) all fresh oil, (2) using depleted oil above TDC of OCR, and (3) using no oil above TDC of OCR

In figure 12, the first solution uses fresh oil above the top-dead-center of the oil control ring. In effect, it assumes that the rings can fully replenish all species of oil lost to vaporization. As such, this solution is an estimate of the maximum vaporization rate given the assumptions laid out in the Model Description section. On the other extreme is the solution using no oil above the TDC of the oil control ring. In this situation, it is assumed that no oil is brought with the rings as they reach the upper part of the ringpack. This solution, therefore, is an estimate for the minimum oil vaporization.

Between the two extremes is the solution where the oil composition is allowed to reach its steady-state value. These are the results produced using the full model presented in Model Description section. Notice how the solutions are smaller than those reported for fresh oil. Any model that does not account for the steady-state oil composition will be over-estimating the oil vaporization rate by more than 30 percentage points. Also notice that as the liner temperature is increased, the depleted-oil vaporization rate becomes smaller (from 85% to 75%) relative to the vaporization rate for fresh oil. This shows that less oil is being vaporized at higher temperatures than

would normally be expected. The oil composition, therefore, must have changed in a way that leads to lower oil vaporization.

Figure 13 shows the estimated distillation curves for the depleted oil at several locations on the liner for the baseline operating conditions. Note that the composition of the fresh Cummins Premium Blue oil is the same as the curve given for the axial location at 100% of stroke. Clearly, the oil in the upper region of the ringpack has been made heavier through the preferential vaporization of its lighter species. In other words, the distillation curve for this oil is shifted due to the depletion of its more volatile species. As a result, less oil vaporizes from the liner than would normally be expected because the steady-state oil composition is less volatile in the upper region of the liner.

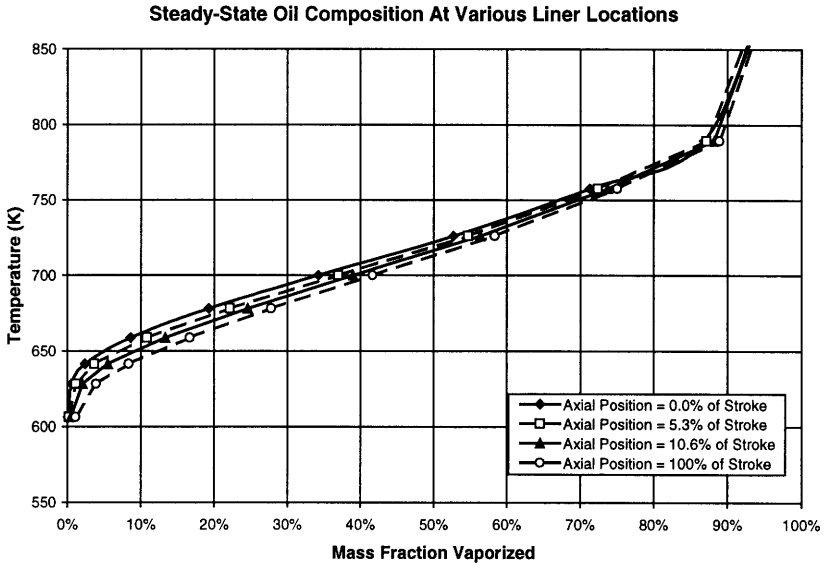

Figure 13: Distillation curves showing estimated steady-state composition of oil at various points along cylinder liner (at baseline conditions)

Presenting this data in another way, figure 14 shows how the average boiling point of the liner oil changes with position. The average boiling point is defined as the point on the distillation curve where 50% of the mass has been vaporized.

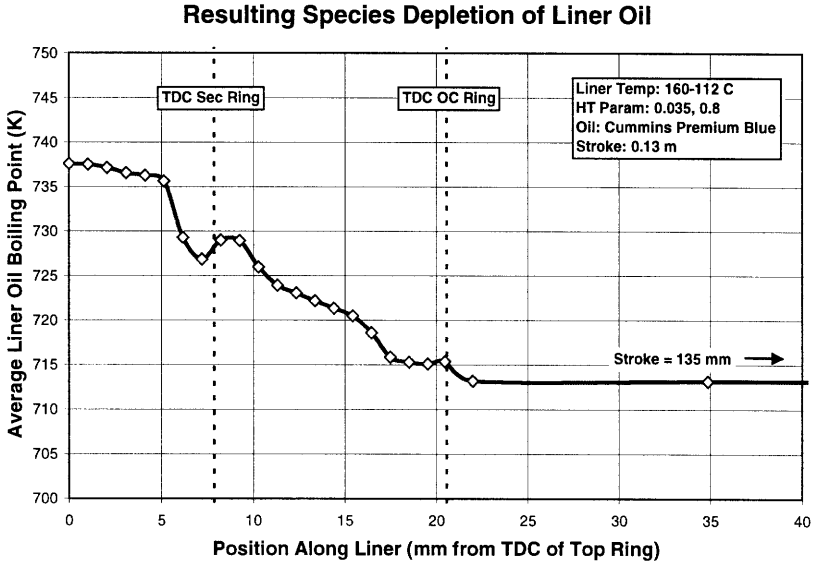

Figure 14: Steady-state, average boiling point of the liner oil at various locations on the liner (baseline conditions)

As can be seen in the above graph, the average boiling point increases significantly on the portion of the liner above the top dead center of the oil control ring. The specific shape of this curve in the upper liner region depends on where the rings release oil. If more oil is released in a given region, the local oil composition is more refreshed, its average steady-state boiling point will be lower, and its overall volatility will be higher. If less oil is released in a given location, the local oil composition will be less refreshed, the local average boiling point will be higher, and the overall volatility will be lower.

To further explore the effects of oil volatility on oil vaporization, results were generated using a different SAE 15W40 oil (see distillation curves, figure 3). This unspecified SAE 15W40 is more volatile than the Cummins Premium Blue used for previous calculations. As expected, total vaporization from the liner is higher. Averaged over the range of temperatures and mass transfer parameters, the unspecified SAE 15W40 is seen to have a vaporization rate 66% higher than that for the Cummins Premium Blue 15W40. The sensitivity to liner temperature, mass transfer parameters, and oil depletion are very similar to those shown in figures 11 through 13 so they are not reproduced here.

Overall, it is expected that an engine in this class will have a total oil consumption rate of 10-13 g/hr/cylinder. For the baseline MT parameters while using the Cummins Premium Blue 15W40, it is seen that oil vaporization contributes about 10% to this overall consumption value. Using the other SAE 15W40 oil, the oil vaporization at baseline conditions is seen to be about 17% of the overall oil

consumption. Therefore, while oil vaporization does not appear to be the dominant source of oil consumption for this engine, it does appear to be a significant source.

3.5. Timing of Vaporization

Also of interest is when vaporization occurs during the cycle. Figure 15 shows the instantaneous total amount of oil vaporized during the cycle normalized by the total amount oil vaporized for the entire cycle. Figure 15 shows results for the baseline operating conditions using the Cummins Premium Blue oil. Notice that most (74%) of the vaporization occurs during the intake and compression strokes (-360 through 0 degrees crank angle). Relatively little vaporization (10%) occurs during the expansion stroke (0-180 degrees crank angle) even though the cylinder gas temperature is much higher.

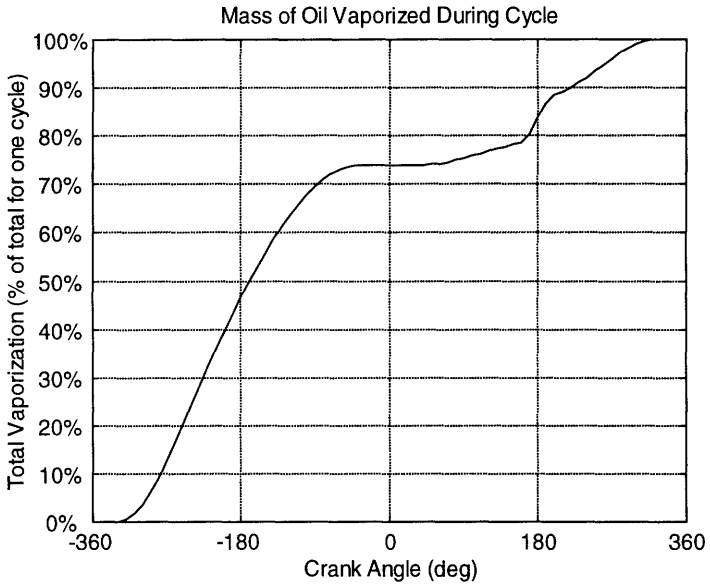

Figure 15: Estimated oil vaporized during one cycle at baseline conditions using Cummins Premium Blue 15W40 oil

One possible explanation for this behavior can be seen by looking at the behavior of various oil and cylinder gas properties as they vary through the cycle and as they affect mass convection. Specifically, examine the temperature trace given in figure 8. The gas temperature is lowest in the intake and compression strokes and highest in the expansion and exhaust strokes. The timing of the vaporization (figure 15) seems to be inversely related to this trend.

Looking at how temperature used to calculate mass convection, it is known that the liner oil temperature is critical to calculating its vapor pressure and, therefore, its surface mass fraction (equation (2)). This mechanism would lead to the belief that cylinder gas temperature is directly

related to vaporization – not indirectly related as suggested by the relation of figure 8 to figure 15. But, looking at the data produced by the model (not shown here), the surface temperature of the liner oil only deviates by a maximum of 5 degrees C from the nearby liner temperature. The temperature of the cylinder gas, therefore, does not strongly influence the temperature of the oil. The influence of the temperature of the cylinder gases on the vaporization rate, therefore, is muted.

Gas temperature also influences oil vaporization through its effect on the cylinder gas properties used in equation (5). Here, temperature is related (along with pressure) to the gas density, gas viscosity, and oil diffusivity. After including the effect of the *a, d,* and *e* parameters of equation (5), it is the inverse relation of temperature to density that is strongest. The strength of the inverse temperature-density relation seems to overcome the negating pressure effects. More work is required to explain this further.

3.6. Dependence of Vaporization on Engine Speed

The last parameter to be examined in this study is the effect of speed on oil vaporization. Figure 16 shows the oil consumption on baseline operating conditions for a range of speeds. In generating this vaporization data at this speed, the cycle simulation, ring pack, and liner oil film thickness models were re-run using the new engine operating conditions. Full load was used for each of the cases.

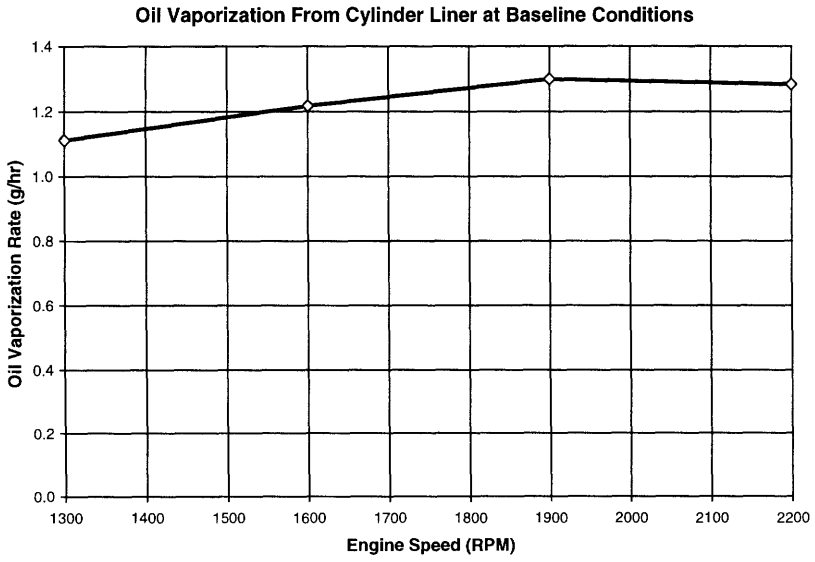

Figure 16: Estimated oil vaporization from cylinder liner at baseline conditions and various engine speeds

As can be seen, oil vaporization is seen to vary about 15% over the range of engine speeds. There seems to be no direct correlation between engine speed and vaporization. This is understandable considering that the engine speed affects so many of the parameters important to the computation of vaporization such as the cylinder gas velocity, the oil film thickness, the ring dynamics, and the rate of oil transport by the rings. Since the influence of engine speed on these individual mechanisms is not well known, then the resulting effect on vaporization is difficult to explain as well.

4. SUMMARY AND CONCLUSIONS

A model has been formulated to estimate the in-cylinder oil vaporization from the liner. It assumes that vaporization is a mass convection process. It accounts for multi-species oil, variable liquid oil properties, variable oil vapor properties, variable cylinder gas properties, and variable liquid oil temperatures. Unlike previously published models, the model presented here also allows the computation of the steady-state oil composition, which may deviate substantially from the default specified oil composition.

The following results are found for a heavy-duty diesel engine running at full load using a SAE 15W40 engine oil:

1. Total vaporization rate was found to account for 10% of the total oil consumption expected for an engine in this class – 1.3 g/hr/cyl out of a total of 10-13 g/hr/cyl.
2. Vaporization was found to be strongly dependent on liner temperature resulting in an order-of-magnitude increase in vaporization for a 38 degrees Celsius increase in liner temperature.
3. Vaporization was found to be strongly dependent on liner oil composition by exhibiting a 66% increase in vaporization simply by switching to a different oil even though the new oil was of the same class.
4. The overall vaporization rate using the computed steady-state oil composition was found to be approximately 75-85% of the rate found using the default (fresh) oil composition.
5. The steady-state liner oil composition was found to have fewer volatile compounds than the default oil composition -- especially that oil which was on the region of the liner inaccessible to the oil control ring.

6. Most of the vaporization was found to occur during the intake and compression strokes (74%).
7. Oil vaporization seems to have little dependence on engine speed.

OIL TRANSPORT ALONG THE LINER - COUPLING LINER OIL VAPORIZATION TO OIL FILM THICKNESS (*FRICTION-OFT*) ANALYSIS

ABSTRACT

Two existing models – a liner oil film thickness / friction model and a liner oil vaporization model – were coupled together. The coupling allowed more accurate estimates of liner oil film thickness, liner oil vaporization, and transport of oil along the liner.

Results are presented for a heavy-duty compression-ignition engine running at 2200 RPM and full load using an SAE 15-W40 class oil. Oil was seen to be brought to the upper part of the cylinder liner (above TDC of OCR) by detaching itself from the faces of the top two rings as they approach TDC. This carrying of oil by the rings was seen to supply about 14 g/hr of oil to the upper liner. Doubling the ring tension of the top two rings decreased this oil supply by 26%. It also increased second ring scraping by 50%. Finally, the decreased oil supply reduced overall liner oil vaporization by a mere 7%. Vaporization from the upper liner, however, was decreased by 23% -- similar to 26% the reduction in oil supply to this region.

1. INTRODUCTION

As seen in the previous sections, the liner oil vaporization model is used in conjunction with the Friction-OFT (liner oil film thickness) model for the purposes of estimating overall oil vaporization. Whenever oil vaporized from the liner, the remaining oil film thickness is smaller than before vaporization. This information was never coupled back into Friction-OFT. As the modeled rings in Friction-OFT returned to the area where vaporization occurred, it did not know that the film thickness should be smaller than the thickness left by the previous stroke. This addendum discusses the results when the liner oil vaporization model is coupled back into the Friction-OFT model.

Also, an application of this model is presented. Specifically, the oil transport along the liner due to ring scraping and carrying is shown. The effect of changing piston ring tension is demonstrated and the resulting effect of lower oil supply on ring-liner friction and oil vaporization is quantified.

2. MODEL DESCRIPTION

The new combined model is composed of (1) the liner oil vaporization model described previously in this report (referred to as LinerOilVap) and (2) the ring-liner friction and liner oil film thickness model created by Tian *et al.* (referred to as Friction-OFT) [1]. Both models perform their simulations on a crank angle by crank angle basis. Integrating the two models, therefore, simply requires that the programming elements of the models be called in the right order. No major restructuring of the existing programming elements or modeling approach is required.

2.1. Implementation of LinerOilVap

The theory of LinerOilVap is described in detail previously. Its implementation is carried out on a crank angle by crank angle basis. Specifically, at every crank angle the vaporization of each liner location is computed. Also the oil refreshing action of the piston rings is also computed at each location passed by the piston rings during that crank angle. As a result, all data generated by the liner oil vaporization model for a given crank angle is available at one time.

2.2. Implementation of Friction-OFT

The Friction-OFT model is also implemented on a similar crank angle by crank angle basis. Each ring, however, is computed separately over a 180 degree stroke. For example, during a piston up-stroke, the top ring is modeled crank angle by crank angle through 180 crank angle degrees. Then, after the top ring has moved from BDC to TDC, the second ring goes through the same process for the same 180 degrees. Finally, the oil control ring is simulated over the same 180 degrees. As a result, Friction-OFT is unlike LinerOilVap in that not all the data generated by Friction-OFT for a given crank angle is available at the same time.

Specifically, if one is interested in the state of the oil film and friction generated by the piston rings at a crank angle of 45 degrees after BDC, then one must wait for both the top and second rings to *complete* the up-stroke from BDC to TDC *and* wait for the OCR to complete the 45 degrees after

BDC before all the data is available. This has implications for integrating Friction-OFT and the liner oil vaporization model.

2.3. Implementing the Model Integration

Because of this discrepancy in the timing of calculations, it is easier to allow Friction-OFT to perform normally and to fit LinerOilVap into Friction-OFT. In any case, it is desirable to modify the two models as little as possible.

To carry out this integration with as little modification as possible to the two models, a new set of code was created to act as an interface between Friction-OFT and LinerOilVap. The interface is called from Friction-OFT at every crank-angle computation by each ring. This added function call in Friction-OFT is the only change required to the code of Friction-OFT.

The interface code handles all the timing differences between the calculation of data in Friction-OFT and the calculation of data in LinerOilVap. The interface also collects the data generated by Friction-OFT and reshuffles it into the format required by LinerOilVap. The reverse process of translating LinerOilVap data into Friction-OFT data structures is also performed by the interface code.

The interface executes the LinerOilVap once all the data necessary to run the model has been computed by Friction-OFT. Specifically, LinerOilVap needs to have the updated liner oil film thickness value for the portion of the liner exposed to the cylinder gasses. These data are only available from Friction-OFT when all three rings are at BDC. The oil film thickness taken from Friction-OFT at this point is used as the initial condition to LinerOilVap for calculations starting at the previous TDC to the following TDC. In this manner, the Friction-OFT and LinerOilVap models are both executed for 360 crank angle degree spans each offset from each other by 180 degrees.

For example, the Friction-OFT may start its computations at -180 degrees CA (with 0 degrees representing TDC at combustion). It will run from -180 degrees through +180 degrees crank angle. Once it has completed its run to +180 degrees, LinerOilVap will be executed so that it runs from 0 degrees CA to 360 degrees CA. Friction-OFT then continues the cycle (using the new liner oil film thickness computed by LinerOilVap as input) by performing computations from +180 degrees CA through +450 degrees CA. This algorithm continues cycle-after-cycle until steady-state is achieved.

The one complicating issue in this scheme is that the LinerOilVap model performs half of its computations *before* the same time-span has been simulated in Friction-OFT. Specifically, the liner

oil vaporization during up-strokes is computed before the liner film thickness data resulting from the up-stroke is computed by Friction-OFT. While the liner oil film thickness data for up-strokes is needed from Friction-OFT, LinerOilVap does need the ring-wetting data generated by Friction-OFT in order to calculate the oil refreshment action by the passing of the rings. This data is not available to LinerOilVap during up-strokes because Friction-OFT has yet to generate the data.

It was decided, therefore, to modify LinerOilVap by extracting the code used to calculate the liner oil refreshment so that it can be called separately from the normal crank angle by crank angle operation of the LinerOilVap model. Once extracted, this new liner oil refreshment module is executed by the interface code described previously. It is called after every 180 crank angle degrees of Friction-OFT computation. As a result, the liner oil film composition is always updated prior to computations in LinerOilVap.

2.4. Capabilities of Coupled Model

In creating the individual models, several potentially restricting assumptions were used to facilitate their development. Coupling the two models removes some of these restrictions.

Specifically, Friction-OFT assumed that whatever oil thickness was left by the piston rings during one stroke remained on the liner and was used as the input to the piston rings during the next stroke. It ignored the fact that oil vaporization will shrink the oil layer between strokes. This has implications not only on the steady-state liner oil film thickness but, since inlet OFT to the rings affects lubricity and outlet OFT, it also has implications to overall ringpack friction and oil transport by the rings. Since LinerOilVap used the data generated by Friction-OFT, it too was affected by this assumption. The coupling removes this assumption.

3. APPLYING THE MODEL: OIL TRANSPORT

Prior to coupling the models, any oil transport analysis on the rings based on data generated by Friction-OFT could only have shown that the rings were pushing (or carrying) oil up and down the liner. Without the outlet that vaporization provides from the piston-ringpack-liner system, oil could come in below the oil control ring but could not go anywhere. Any discussion of *net* oil transport would be meaningless in this context. Including oil vaporization provides an outlet for the oil from the system. With this outlet, it is possible to have a net transport of oil from the lower, cooler regions of the liner up to the more oil-starved, hotter region of the upper liner where more of the vaporization

occurs. Examining the rate of oil transport along the liner and its effect on oil vaporization and ring-liner friction is purpose of this study.

3.1. Modes of Oil Transport In Piston-Ringpack-Liner System

There are many mechanisms that cause liquid oil to be moved around in the Piston-Ringpack-Liner system (figure 17). Driving mechanisms include inertia, ringpack gas flows, pumping motions by rings, scraping of oil from the liner by the rings, and carrying of oil along the liner by the rings. Paths for oil transport include transport along piston lands, through ring gaps, into and out of ring grooves, and along the cylinder liner. Given that several mechanisms can drive oil along each of the several paths, quantifying oil transport in this system is very complicated.

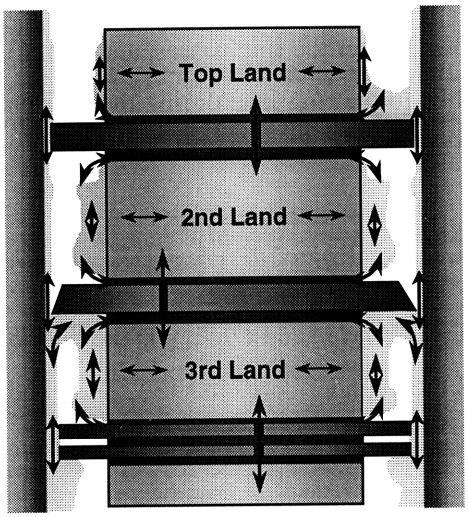

Figure 17: Some possible modes of oil transport in the piston-ringpack-liner system

3.2. Focussing On Scraping and Carrying By The Rings

Based on the data generated by the coupled Friction-OFT and LinerOilVap models, two of the oil transport modes introduced above can be examined quantitatively – scraping and carrying by the rings.

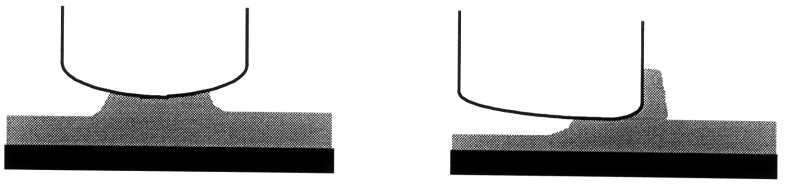

Carrying

Oil attached to ring face can be carried from one part of liner to another

Scraping

A flooded ring can scrape oil thereby limiting how much is left on the liner

Figure 18: Carrying and scraping as possible modes of oil transport

Scraping is defined to occur when oil on the liner floods the leading edge of the ring face (figure 18). The rate of oil being removed from the cylinder liner due when the leading edge is flooded (minus the change in volume being carried) is called the scraping rate. The scraping rate at a given location can be computed by (1) looking at the amount of oil on the liner before the ring passes, (2) subtracting off the amount of oil left on the liner after the ring passes, and then (3) subtracting off the amount of additional oil that became attached to the ring face during the ring passing. Defined more precisely, the volume rate of oil scraping, $Q_{scraped}$, can be found from:

$$Q_{scraped} = Vel_{piston} * \left(OFT_{before} - OFT_{after}\right) * bore * \pi - \frac{d\left(Vol_{\text{under ring}}\right)}{dt} \tag{10}$$

where Vel_{piston} is the instantaneous piston velocity, OFT_{before} and OFT_{after} is the liner oil film thickness before and after the passing of the ring, *bore* is the cylinder bore, and $Vol_{under\ ring}$ is the volume of oil carried the ring face.

Oil carrying occurs because oil attaches itself to the ring face as the ring moves up and down the liner (figure 18). The oil attachment occurs because it is assumed that there is a no-slip condition in effect between the oil layer and the ring face. As a result, oil is dragged up and down the liner as the ring itself moves up and down the liner. At any given moment in time, a certain volume of oil is trapped under the ring face and is being carried with the ring. To calculate the amount of oil attached to the ring face (and, therefore, oil transported by carrying), calculate the volume of oil under the ring face and then, to account for the amount of oil *not* moving with the ring face, subtract off the volume of oil left on the liner after the ring passes. The remaining volume is defined as the carried oil (figure 19). All of the data necessary to calculate these volumes are provided by Friction-OFT.

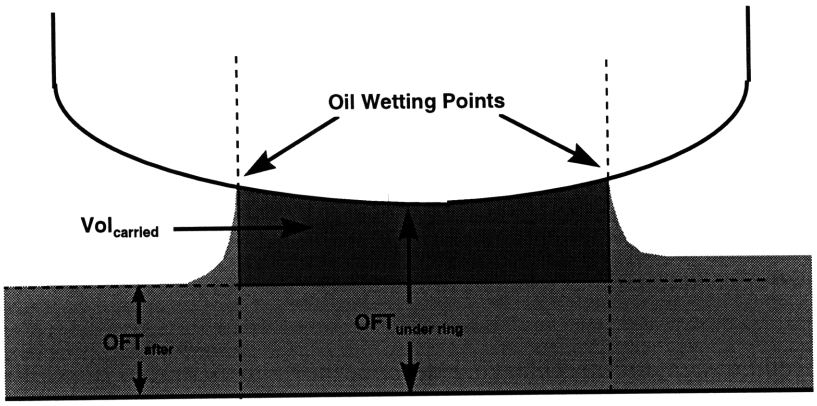

NOTE: Must account for instantaneous ring twist (coordinate transformation)

Figure 19: Definition of volume of oil carried with ring face. Use *Friction-OFT* to find oil wetting points, $OFT_{under\ ring}$, and $OFT_{after\ ring}$,. Knowing the profile of the ring face, integrate to find the area under ring face while accounting for ring twist and subtracting oil remaining on the liner after the ring passes.

An algorithm for computing the amount of oil being carried is complicated by the fact that the oil has a dynamic ring twist. Therefore, a coordinate transform has to be embedded has to be performed to account for the fact that the shape of the ring face is defined in one coordinate system while the area under the ring face must be computed in a different (rotated) coordinate system. The algorithm presented below performs three steps: (A) integrates to find the area of oil under the wetted portion of the ring face in the ring's coordinate system, (B) adds a given amount of area to account for the instantaneous height of the ring above the liner, (C) transforms the coordinates of the wetting boundaries, and (D) adds or subtracts area to account for the instantaneous ring twist:

$$Area = \int_{XL}^{XU} f_{RingFace}(x)dx + \frac{h_0}{\cos(\theta)}(x_U - x_L) \tag{11A}$$

$$\begin{aligned} h_u &= f_{RingFace}(x_U) + h_0 / \cos(\theta) \\ h_L &= f_{RingFace}(x_L) + h_0 / \cos(\theta) \\ h_U^* &= x_U \sin(\theta) + h_U \cos(\theta) \\ h_L^* &= x_L \sin(\theta) + h_L \cos(\theta) \\ x_U^* &= x_U \cos(\theta) + h_U \sin(\theta) \\ x_L^* &= x_U \cos(\theta) + h_L \sin(\theta) \end{aligned} \tag{11B}$$

$$\frac{Vol_{carried}}{Bore * \pi} = Area - \frac{\tan(\theta)}{2}(h_U^2 - h_L^2) + \frac{\tan(\theta)}{2}(x_U^2 - x_L^2) \tag{11C}$$

where $f_{RingFace}(x)$ is the defined shape of the ring face in a coordinate system attached to the ring, h_0 is the instantaneous height of the ring's coordinate origin above the cylinder liner, θ is the instantaneous rotation of the ring (positive rotation raises leading edge on up-strokes), x is the horizontal position of

the location of the wetting point of the ring face relative to the ring's coordinate system, and h is the vertical position of the location of the wetting point of the ring face relative to the ring's coordinate system. The subscripts U and L refer to the upper and lower wetting points (up is closer to the combustion chamber). The star superscript ("*") refers to the wetting position in the frame of reference of the cylinder liner. Note that the wetting positions (x_U and x_L), the height of the ring (h_0), and the ring twist (θ) are all outputs given by Friction-OFT.

Taken together, scraping and carrying describe how oil is moved along the cylinder liner. Understanding how oil moves along the cylinder liner will help to understand how oil moves from the oil-flooded lower region of the liner where the oil control ring is able to reach and the oil-starved upper region of the liner where the oil control ring cannot reach.

Also, understanding when scraping occurs and how much oil is removed from the liner can be the first steps to understanding one of the ways that liquid oil gets into the ring grooves and onto the piston lands. Scraping may be the main source of oil supply to the upper ring pack. Knowing the scraping rate may help to understand the amount of oil that may be resident in the ringpack, how much oil vaporizes from the ringpack, and how much oil degradation and deposits form on the piston and rings.

3.3. Plan for Studying Scraping and Carrying

To examine the amount of scraping and carrying present in a typical diesel engine, it was decided to apply the coupled Friction-OFT/LinerOilVap model to the same Cummins diesel engine as modeled previously. Since the liner is well supplied with oil wherever the oil control ring can reach, this study focuses on quantifying oil supply to the region of the liner above the top dead center of the oil control ring. Also, the rate of scraping along the entire liner is also quantified.

In the field, the easiest means to affect oil supply to the cylinder liner is to adjust the tension of the piston rings. Since this is a study on oil transport and oil supply on the liner, the effects of varying ring tension are simulated using the coupled model. The resulting oil transport rates are presented and the subsequent effects on oil vaporization from the liner and ring-liner friction are also shown.

4. RESULTS AND DISCUSSION

4.1. Description of Engine and Baseline Case

To generate the results generated in this section, the same Cummins diesel engine is simulated as in the prior sections (table 1). Also the same 2200 RPM, full load baseline operating condition used in the previous sections was used as the baseline case for this study (table 2). The oil used is the same Cummins Premium Blue SAE 15W40 oil used in previous simulations (figure 3). Additional information on the piston rings used in the simulations is shown in table 3 below.

Table 3: Description of piston rings used in simulations

Top Ring	Barrel-Faced (worn profile)
Second Ring	Taper-Faced (worn profile)
Oil Control Ring	Single Barrel-Faced Rail[1]
Top Ring Tension	22 N
Second Ring Tension	20 N
OC Ring Tension	90 N

4.2. Transport to Upper Liner By Carrying

To illustrate how oil is carried to the upper liner through oil being carried by the piston rings, examine figure 20(A) that shows how, in certain regions, more oil is left after a ring passes than was there before the ring passed. In this particular case, the graph shows how the top ring affected the liner oil film thickness during the compression stroke. Figure 20(B) shows the ring wetting condition for the top ring during the compression stroke. Notice that the ring face is most wet during the middle portions of the stroke when the oil film thickness is highest and that the ring becomes much less wet as the oil film thickness becomes thinner at top dead center

[1] While the actual oil control ring is a two-piece ring, the current implementation of Friction-OFT cannot accept this geometry. By adjusting the size and shape of the fictitious single rail OC ring used here, the behavior of a typical two-piece ring is simulated as closely as possible.

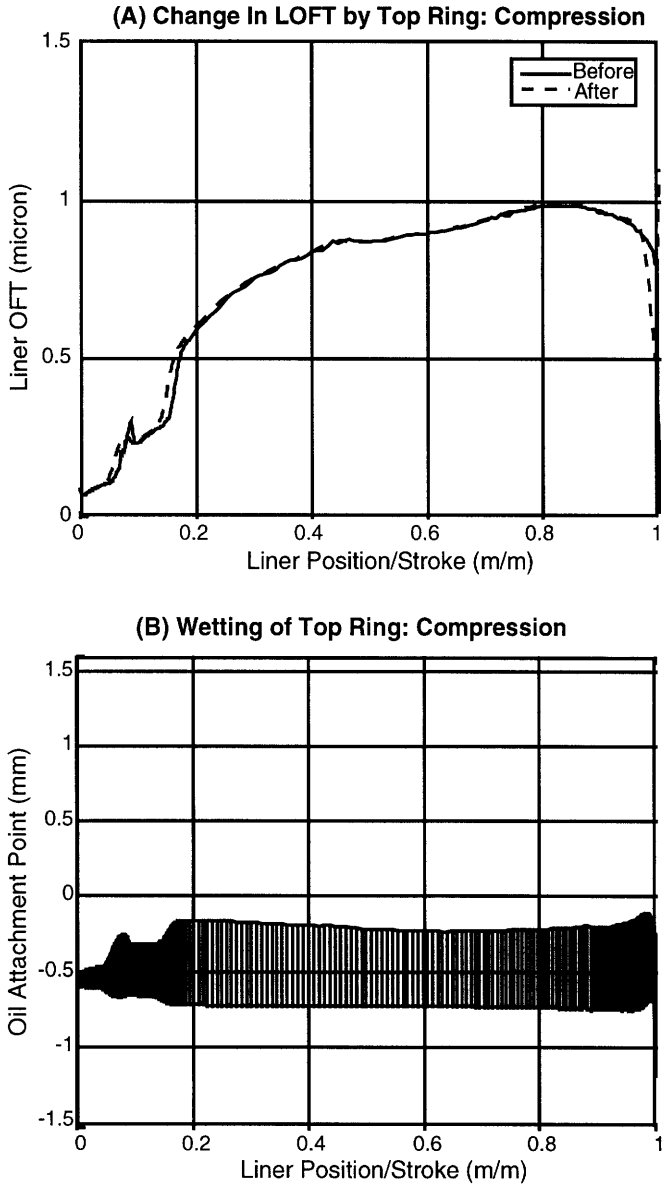

Figure 20: (A) Change in liner oil film thickness by the top ring during compression stroke and (B) the ring's instantaneous wetting condition. Full load, 2200 RPM.

Figures 21(A) and (B) represent the same data zoomed in to examine the behavior above the TDC of the oil control ring. Notice in figure 21(A) that the ring is clearly adding oil to the liner as it moves toward TDC -- the oil film thickness after the ring passes is higher than before the ring passes. The theory that the rings supply oil to the upper ring pack is demonstrated in this graph.

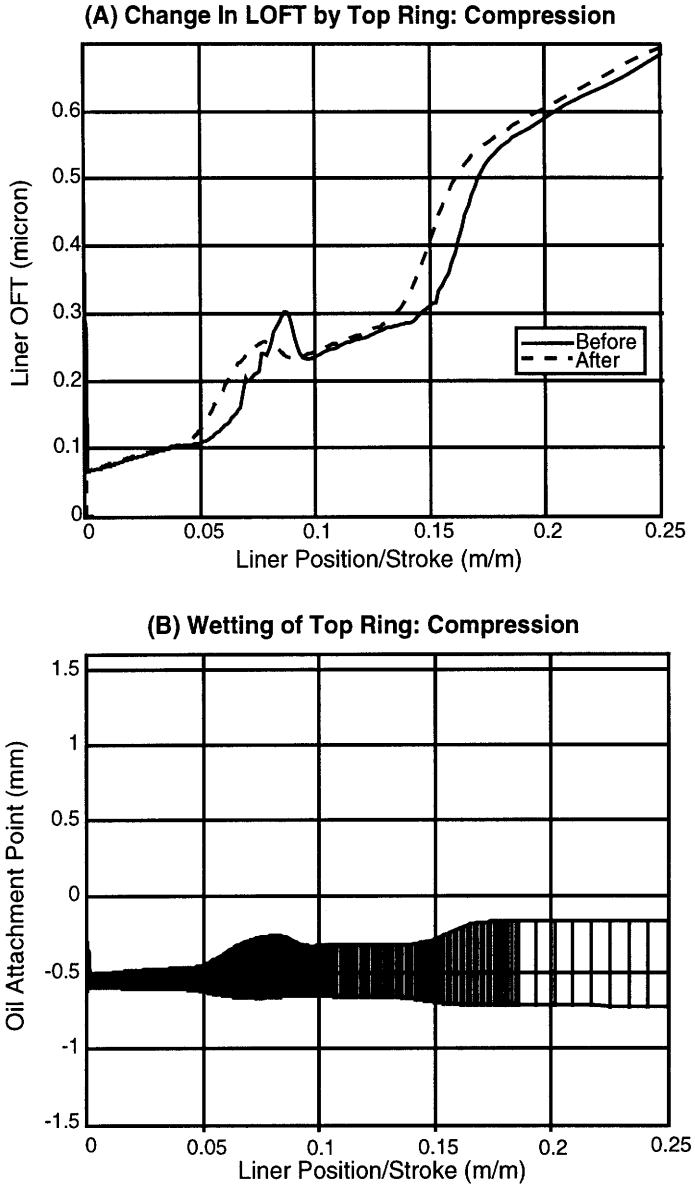

Figure 21: (A) Zoom of change in liner oil film thickness by the top ring during compression stroke and (B) zoom of the ring's instantaneous wetting condition. Full load, 2200 RPM.

Also, in figure 21(A), notice that as the ring moves toward TDC, it is closing toward the liner. From the ring's perspective, its height above the liner is shrinking. At the same time, as seen in the ring wetting graph (figure 21(B)), the wetted area of the ring is shrinking. Taken together, this means that the total volume of oil under the ring face (e.g. the oil *carried* with the ring) is shrinking. Since mass must be conserved, the amount of oil that is not longer being carried with the ring face is being released to the liner. So, oil carrying by the rings acts to bring oil to the upper part of the liner.

4.3. Quantifying Oil Supply Due to Carrying by Rings

To quantify the amount of oil supplied to the upper liner due to carrying by the rings, it is necessary to quantify the amount of oil carried with the rings as they cross into the upper part of the liner. However much oil is being carried with the rings as they pass the TDC of the OCR is all the oil available to be redepositted on the upper portion of the liner. Granted, as the rings move back down to the lower part of the liner, they will be carrying some oil with them. Therefore, not all the up-carried oil actually gets redepositted. Still, even is some of the oil is carried back out of the region, the entirety of the up-carried oil is available to the upper liner and it does act to partially refresh the composition of the oil on the upper-liner.

A value for the oil supply to the upper liner is computed by calculating the oil carried by each ring (figure 19) as it crosses the TDC of the OCR. For this engine, the TDC of the OCR is 20 mm from the TDC of the top ring. The total oil supply to the upper liner at the baseline operating conditions including the influence of both the compression and exhaust up-strokes is shown in table 4.

Table 4: Oil supply to upper liner at baseline conditions

Top Ring	5.44 g/hr
Second Ring	4.14 g/hr
Total Oil Supply	**9.58 g/hr**

4.4. Effect of Ring Tension On Oil Supply To Upper Liner

In practice, ring tension is generally used to control oil supply to the liner as well as to control ring-liner friction and oil consumption (through vaporization and other mechanisms). To observe how the coupled Friction-OFT/LinerOilVap model would respond to such a change, the tension of the top and second rings were doubled to 44 N and 40 N respectively.

The effect on liner oil film thickness is clear – figure 22 shows that higher ring tension causes the oil film to be thinner. After the expansion stroke, the oil film is an average of 24.9% thinner using double tension. After the intake stroke, the oil film is an average of 20.0% thinner using double tension.

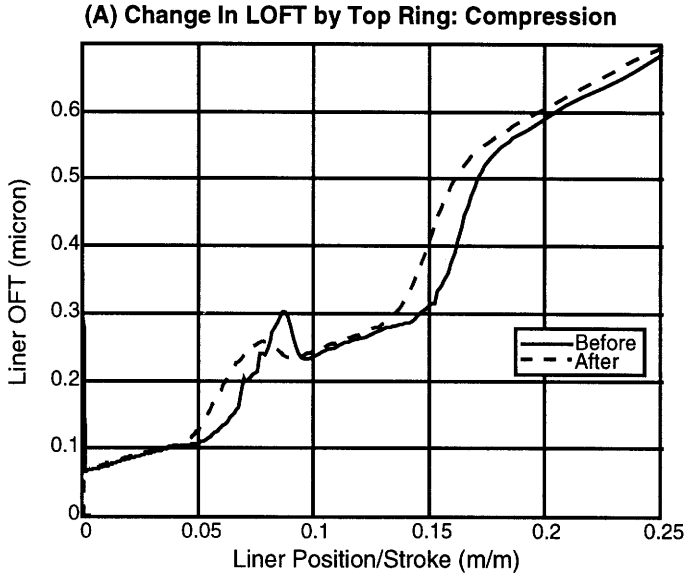

Figure 22: Effect of ring tension on liner oil film thickness at full load, 2200 RPM

Looking at figure 23, it is seen that even with double tension, the top ring still leaves extra oil behind on its upstroke. It still carries oil to the upper part of the liner. As a side note, the graph shows that the oil film thickness goes to zero close to TDC. This does not necessarily mean that there is not oil. Since the root-mean-square of the liner surface roughness in all of these cases is 0.15 microns, any oil film thickness below 0.15 (including a value of zero thickness) has little meaning.

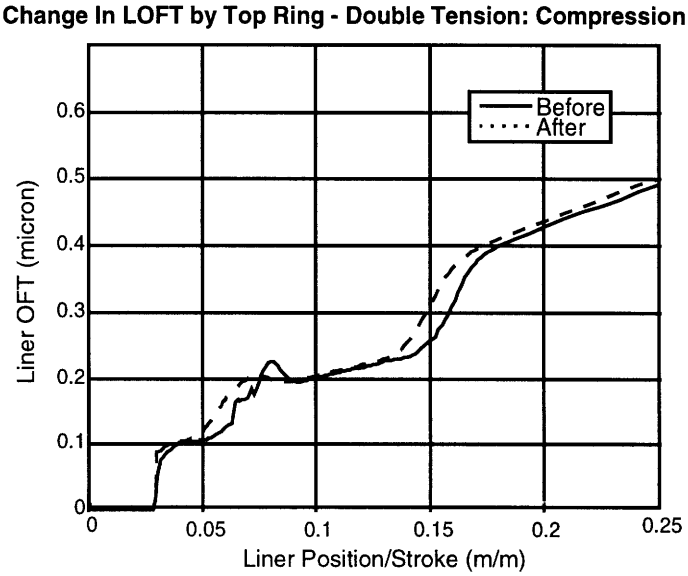

Figure 23: Change in liner oil film thickness by the top ring during compression stroke. Full Load, 2200 RPM, Double Ring Tension.

By taking the difference in the before and after oil film thickness displayed in figure 23, the location and amount of oil release by the top ring can be easily seen. Figure 24 shows the location

and amount of oil release by the top ring for both normal and double ring tension. Notice that oil is released in similar locations for both levels of tension, yet less oil is released to the liner for the double tension case.

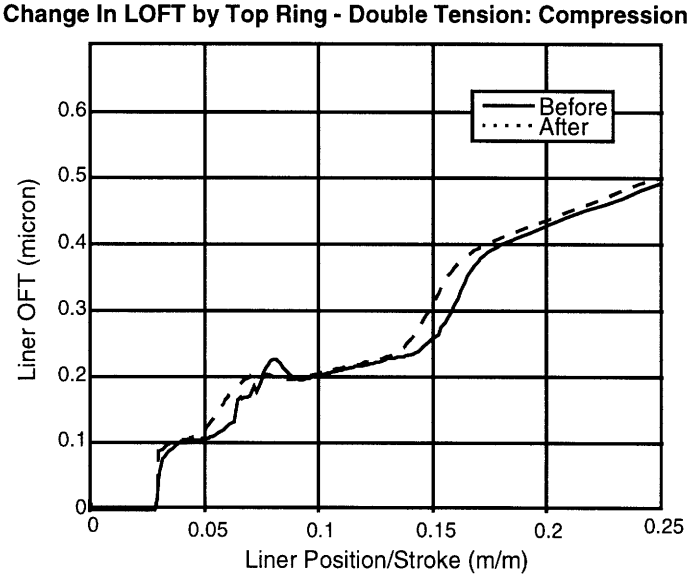

Figure 24: Effect of ring tension on the amount and location of oil released from top ring to the liner during the compression stroke. Full Load, 2200 RPM.

Using the same procedure to quantify oil supply as used earlier, the effect of ring tension on oil supply can be seen in Table 5. Clearly, doubling the ring tension decreases the oil supply to the upper liner significantly.

Table 5: Effect of ring tension on oil supply to upper liner due to carrying by rings

Ring Tension	Top Ring (g/hr)	Second Ring (g/hr)	Total (g/hr)
Normal Tension	5.44	4.14	9.58
Double Tension	3.79	3.44	7.23
Total Change	**-30.3%**	**-16.9%**	**-24.5%**

4.5. Quantifying Scraping and the Effect of Ring Tension

As described previously, scraping occurs when the leading edge of a ring becomes flooded thereby causing any additional oil on the liner (beyond that required to flood the ring) to be removed from the liner. Looking at figures 25(A) and (B), it is clear that on the expansion stroke (a down stroke), the lower edge of the scraper ring becomes flooded at about 20% of stroke. The result, as seen in figure 25(A), is that the oil film thickness after 20% of stroke becomes much thinner due to the scraping action of the scraper ring.

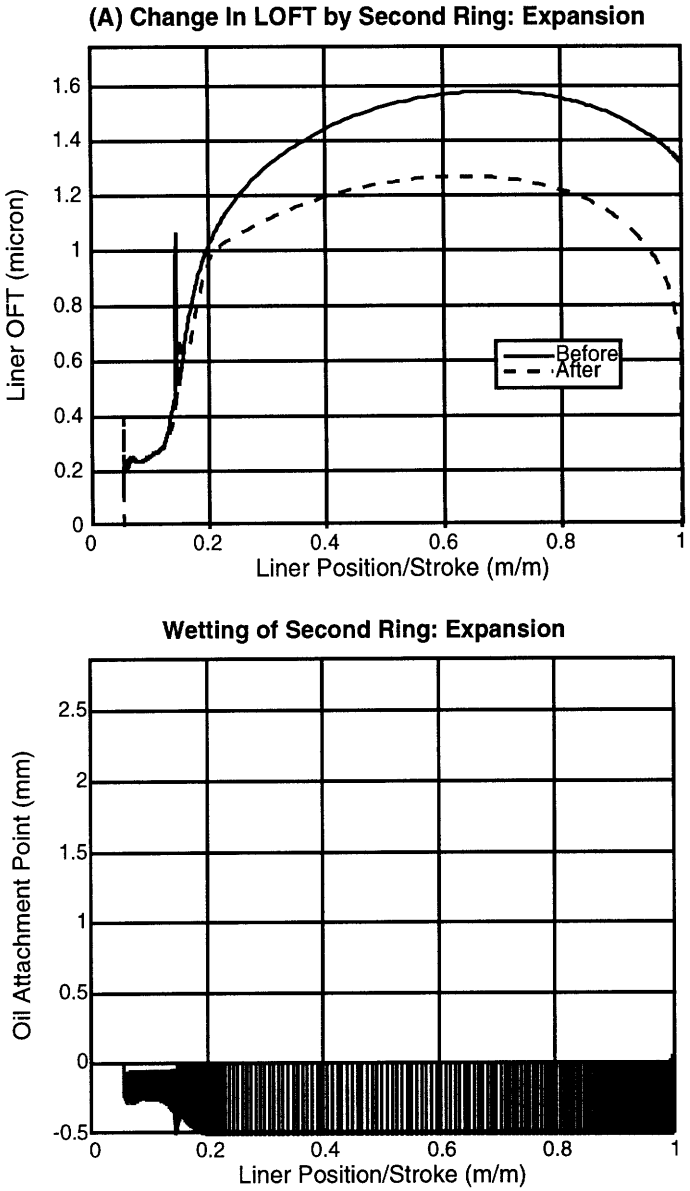

Figure 25: (A) Change in liner oil film thickness by the scraper ring during the expansion stroke and (B) the ring's instantaneous ring wetting condition. Full load, 2200 RPM.

Using equation 10, the scraping rate can be computed on an instantaneous basis. The term for the change in volume of oil stored under the ring can be computed numerically by computing the oil carried by the ring (figure 19) for each time step and then performing the derivative numerically. The results are presented below in figure 26. Note that the scraping rates have been normalized by the circumference of the cylinder.

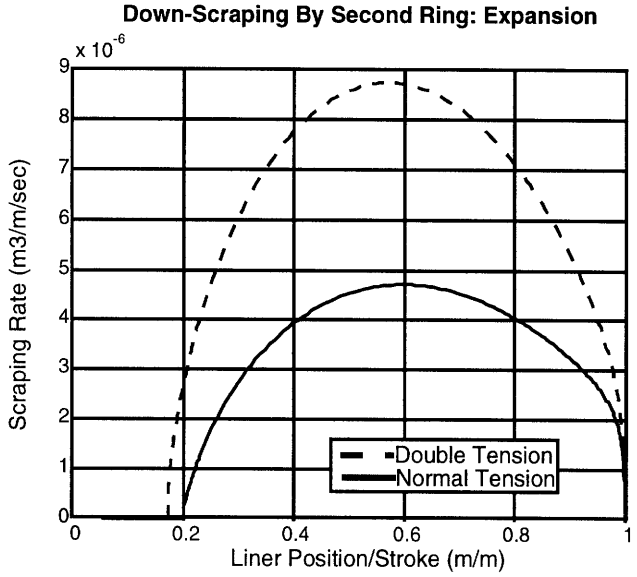

Figure 26: Instantaneous scraping rate by the second ring during the expansion stroke and the effect of ring tension on scraping. Full Load, 2200 RPM.

Figure 26 also shows the effect of ring tension on the scraping rate. It is apparent that, at least during this stroke, increasing the ring tension greatly increases the amount of oil scraped. This could have important implications for oil supply to the ringpack since scraped oil could be a major source of oil to the piston lands and ring grooves.

Taking a time average of the scraping rate over a full 720 degree four-stroke cycle, an average scraping rate is found for each ring. Note that for this engine under these running conditions, there was no up-scraping by either ring and that there was no scraping at all by the top ring. Also, there was no scraping to or from the upper region of the liner. The table below summarizes the scraping results and the effect of doubling the tension.

Table 6: Average rate of down-scraping by top two rings and the effect of ring tension. Full Load, 2200 RPM

Ring Tension	Top Ring (g/m/hr)	Second Ring (g/hr)	Total (g/hr)
Normal Tension	0	2070	2070
Double Tension	0	3160	3160
Total Change	**0%**	**+52.7%**	**+52.7%**

Note that magnitude of the scraping rates are in *thousands* of grams per hour. Scraping rates, therefore, are several orders-of-magnitude higher than the rates for oil carrying and for oil vaporization from the liner reported earlier in this report.

4.6. Effect of Ring Tension on Friction

If the goal of adjusting ring tension is to control oil supply to the ringpack and liner and to control oil consumption from the engine, the unwanted side-effect of increased ring tension is increased engine friction. Calculating ring-liner friction was one of the original purposes during the creation of the Friction-OFT model. Friction-OFT includes numerous effects when calculating friction including hydrodynamic, boundary and mixed lubrication conditions. In boundary and mixed lubrication conditions, Friction-OFT includes the effects of liner and ring face roughness. Friction-OFT also includes the temperature and shear-rate dependent behavior (e.g. the non-Newtonian fluid behavior) of the lubricating oil.

Using the Cummins Premium Blue oil and using viscosity and non-Newtonian fluid parameters consistent with an oil of this class, the mean effective friction pressure (FMEP) for the total ringpack was found to be 11.69 kPa using normal ring tension. Doubling the ring tension increased this value 16.3% to 13.58 kPA.

4.7. Effect of Ring Tension on Oil Vaporization

Since changing the ring tension also affects oil supply to the liner (see section 4.4 above), changing the ring tension will also have an effect on oil vaporization from the liner (oil supply affects oil composition and oil composition affects liner oil vaporization – sections 2.7 and 3.4 in the previous study in this report). Table 7 below shows how vaporization is affected by ring tension.

Table 7: Effect of ring tension and oil supply on liner oil vaporization rates.

Ring Tension	Oil Supply To Upper Liner (g/hr)	Vap From Above TDC of OCR (g/hr)	Vap From Below TDC of OCR (g/hr)	Total Vaporization (g/hr)
Normal	9.58	0.475	1.142	1.617
Double	7.23	0.364	1.139	1.503
Total Change	**-24.5%**	**-23.42%**	**-0.22%**	**-7.04%**

In this data, notice that the overall vaporization rate only changes by 7%. For most of the liner, however, it was seen that composition of the oil is mostly unchanged (figure 14) therefore oil transport plays little role in liner oil vaporization for most of the liner. The only region where oil supply is important is in the upper part of the liner (above TDC of the OCR) where lower oil supply causes the composition of the oil to change. Changing the oil supply rate to this area should, therefore, change the oil composition in this area and change the resulting oil vaporization from this area. Referring back the table, the model does reflect this coupling. The lower oil supply to the

upper liner at high ring tension (24.5% lower) is seen to have a nearly equal effect on decreasing oil vaporization from this region (23.4% lower).

Finally, note that the vaporization from the upper part of the liner is just a small fraction of the oil supplied to the upper part of the liner. At both normal and double ring tension, only 5.0% of the oil supplied through carrying is lost due to oil vaporization. Most of the oil that is carried up by the rings on the up-strokes, therefore, must then be carried down by the rings on the down-strokes. Like the tides of the ocean, oil flows into the upper liner with the up-strokes and then flows back out with the down-strokes.

Even though oil vaporization is only a small fraction of the oil supply, changing the oil supply still strongly changes the oil vaporization because the oil brought up to the upper liner is relatively fresh oil. This fresh oil mixes with the oil already on the liner (oil that is depleted of volatile species) thereby changing its composition. On the following down-stroke, the ring picks up nearly the same *volume* of oil and carries it back to the lower liner, but, the composition of the down-stroked oil is very different from the composition of the up-stroked oil. While the up-stroked oil came from the lower liner, the down-stroked oil comes from the upper liner. As a result, the down-stroked oil has a lower concentration of light (volatile) species and a higher concentration of heavy (less volatile) species relative to the up-stroked oil. Looking at the data for the top ring at normal ring tension during the compression and expansion strokes, the up-stroked oil has a mean boiling point of 713.2K while the down-stroked oil has a mean boiling point of 715.2K (fresh oil has a mean boiling point of 713.1K as modeled). Therefore, the data shows that lighter oil is carried upward and heavier oil is carried downward.

So, despite the fact that most of the *volume* of oil supplied to the upper liner is just carried back to the lower liner, oil carrying still has an impact on the composition of the oil on the upper liner. More oil carrying by the rings results in more of the light species being transported upward. More light species available results in more vaporization. This coupling between oil supply and liner oil composition of the upper liner is how oil transport seems to affect oil vaporization.

5. SUMMARY AND CONCLUSIONS

To perform a physically appropriate analysis of oil transport along the liner, the liner oil film thickness model, Friction-OFT, and the liner oil vaporization model, LinerOilVap, were coupled together. With the coupled model, oil transport along the liner could be examined without assuming

that the oil vaporization rate relative to the oil transport rate was small. Also, the resulting influence of oil transport rates on oil vaporization could now be studied.

Simulations were run for a heavy-duty diesel engine running at full load and 2200 RPM using a SAE 15W40 engine oil:

1. Oil was seen to be transported to the upper liner (above TDC of the OCR) by being attached to the ring face as the ring moves from the lower liner to the upper liner. This behavior is called oil "carrying" by the ring.
2. Total oil supply to the upper liner was estimated to be 9.58 grams per hour
3. By doubling the tension of the top two rings, the oil supply to the upper liner was reduced by 25%.
4. By doubling the tension on the top two rings, the down-scraping by the scraper ring was seen to increase 53 % from 2070 g/hr to 3160 g/hr. No scraping occurred in the upper liner.
5. By doubling the tension on the top two rings, the ring-liner friction was seen to increase 16.3% (from 11.7 kPa to 13.58 kPa).
6. The increased ring tension and decreased oil supply also decreased total oil vaporization from the liner by 7%. From the upper liner, however, the vaporization was decreased 23.4%. The decrease in vaporization in this region is very similar to the decrease in oil supply to this area. There could be a strong coupling between those two parameters.
7. The oil vaporization rate from the upper liner is about 5% of the rate of oil supply to the upper liner.

ESTIMATING OIL VAPORIZATION FROM THE RINGPACK

ABSTRACT

A model has been developed for estimating the amount of oil consumed due to vaporization from the surfaces of the sides of the piston, the rings, the ring grooves, and the nearby cylinder liner for a reciprocating engine. The model uses input from an external gas dynamics model and computes how oil vapor is convected into the gas stream and subsequently transported about the system so that it eventually reaches the combustion chamber and is lost.

Computer model results are presented for a heavy-duty compression-ignition engine running at 2200RPM and full load. Depending on the mean boiling point of the oil used in the simulation, the oil consumption results ranged from excessive (27 g/hr/cylinder) to insignificant (0.38 g/hr/cyl). The expected total oil consumption for this engine is 10-13 g/hr/cyl. Using an oil boiling point of 775K, the consumption due to vaporization from the ringpack was found to be 3.6 g/hr/cyl (30% of total). For this case, it was found that most of the oil was vaporized from the top of the top ring groove. The rate was so high that this region may become completely dried of oil thereby breaking one of the fundamental assumptions of the model.

1. INTRODUCTION

In the pursuit of quantifying oil consumption from internal combustion engines, many oil consumption mechanisms must be addressed. One mechanism, oil vaporization, has received much attention both in this study and in literature [1][2][3]. That attention, however, has been focused mostly upon oil vaporization from the cylinder liner. Vaporization from the cylinder liner is certainly significant but it is not the only source of oil vaporization. Any surface wetted with oil can vaporize oil. Building on the tools developed to estimate vaporization from the cylinder liner, it should be possible to estimate the vaporization from these other surfaces.

In addition to the cylinder liner, it is possible that vaporization of oil from the piston crevices and from the piston rings may be a significant contributor to overall oil consumption. Following the model used for estimating oil vaporization from the cylinder liner, oil vaporization can occur as long as there are (1) a supply of liquid oil to generate oil vapor and (2) a quantifiable flow of gas to convect away the vaporized oil. The piston ringpack has both.

In terms of liquid oil supply, the oil control ring is likely to be flooded with oil. The purpose of the ring is to govern the amount of oil left on the cylinder liner as the piston moves on its down-stroke. For the ringpack, though, it is certainly possible that oil can work its way from the oil control ring (and its oil-flooded groove) up the sides of the piston so that the rings and crevices of the ringpack become wetted with oil. Also, any oil scraped from the liner by the compression ring or the scraper ring could add to this oil supply. From a qualitative standpoint, therefore, it is reasonable to assume that there is liquid oil in the ringpack available for vaporization.

As for the flow of gas through the ringpack, the high pressures generated in the combustion chamber can force gas to flow down though the ringpack and into the crankcase ("blow-by"). Also, gas can flow in the reverse direction once the pressure in the combustion chamber drops ("reverse blow-by", see Figure 27).

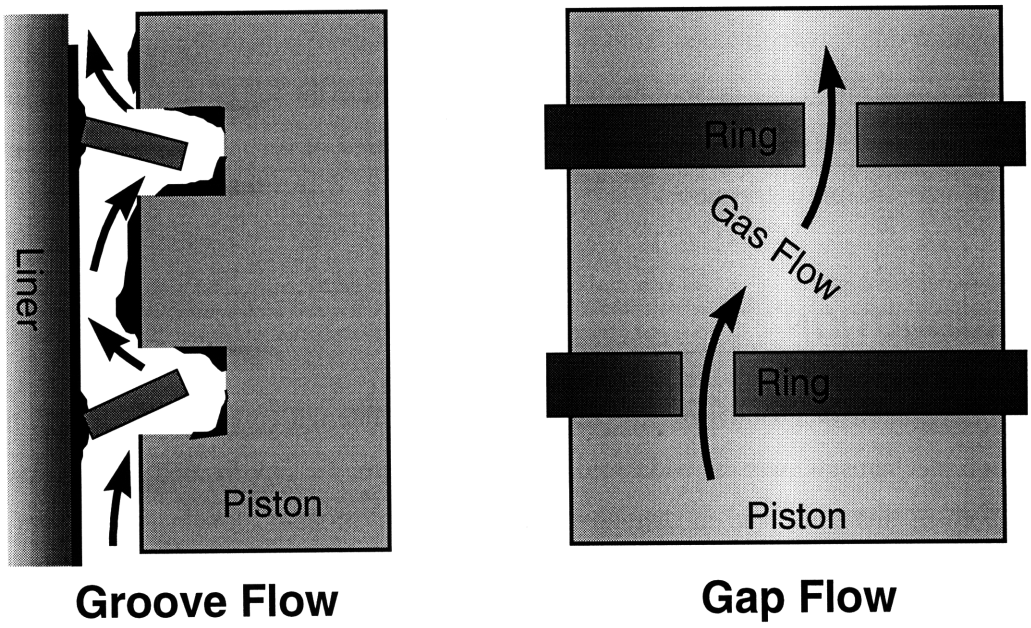

Figure 27: Depiction of two modes of gas flow in the piston ringpack: (A) flow through the ring grooves and (B) flow through the ring gaps

As is shown in the figure, there are two main paths for gas to flow – through the gaps in the rings and behind the rings in the ring grooves. Since any of these surfaces could be wetted with oil, all

combinations of gas flow paths must be considered when analyzing the transport and generation of oil vapor. Luckily, a previous MIT model, Ringpack-OC [4], can already perform all the gas flow calculations. Therefore, a vaporization model only needs to address the physics of convection and the accounting for liquid and vaporous oil.

1.1. Bounding Calculations

It is known from previous studies [5], that the gas in the ringpack does in fact contain some oil. The researchers found that, by weight, the gas in the ringpack contained between 0.5% and 1.0% oil by weight for their 2.2 liter, 1-cylinder Diesel engine. Combining this with our knowledge of gas flow through the ring pack and it is possible to make a quick estimate as to the amount of oil being carried out of the ringpack.

Using Ringpack-OC to simulate the behavior of the same 1.4 L/cylinder Cummins engine modeled previously in this report, the total amount of gas blowing from the ringpack back into the combustion chamber is estimated to be 19 kg/hr/cylinder. Assuming that this gas is 0.5-1.0% oil as suggested by Burnett et al. [5], the total amount of oil being carried from the ringpack to the combustion chamber is 95-190 g/hr/cylinder. Since the expected total oil consumption for this engine is 10-13 g/hr/cylinder, the 95-190 estimate is obviously very wrong. But, that value does show that oil carried from the ringpack by the gas flow could be a significant (and dominant) source of oil consumption from this engine.

This result, however, speaks nothing as to how much oil is *vaporized* from the ringpack. It merely describes how much oil might be *carried* from the ringpack due to gas flow. To be carried by the gas flow, the oil could either be in the vapor form (a gas state), or, it could be in the form of liquid droplets or as a mist (also a liquid state). The generation of oil vapor and the generation of oil mist are two different physical mechanisms and need to be considered separately. Since oil vaporization is the target of the current study, mist will be ignored presently.

To obtain a more realistic estimate for the oil lost due to vaporization, it can be assumed that all gas leaving the ringpack is fully saturated with oil vapor. Using the same Cummins engine as before, a volumetric flow rate for the reverse blow-by is estimated to be 0.187 m^3/hour. If a representative temperature of the gas leaving the ringpack is assumed to be approximately 520K (the average of the crown land temperature and the adjoining liner temperature) and if the oil is assumed

to have a simple boiling point[2] at 715 K (the 50% point on the distillation curve for the oil), then the total amount of oil vapor that could blow from the ringpack to the combustion chamber is approximately 6.27 grams/hour. Given that the expected total oil consumption for this engine is 10-13 g/hr, oil vaporization from the ringpack could be a significant contributor to the overall consumption.

1.2. Purpose of Modeling Oil Vaporization from the Ringpack

The purpose of modeling oil vaporization from the ringpack is to estimate the total amount of vaporized oil that is carried to the combustion chamber during the steady-state operation of the engine. The model is to be used so that the influence of the various engine design and operating parameters on the oil vaporization can be ascertained.

Specifically, using as input the detailed results from the RINGPACK-OC gas dynamics model, this oil vaporization model should compute the amount of oil vapor generated in specific regions of the ring-pack, the amount of oil vapor transported between regions of the ring-pack, and the amount of oil vapor consumed by transport to the combustion chamber.

In terms of fidelity, it is desired to have this model be able to generate results that correctly identify the *trends* of the vaporization behavior. Being an analytical model, much intermediate data about the system can also be generated and seen by the analyst. The details of these intermediate results may be of interest but, since their accuracy was not the goal during the model's development, they may not be entirely self-consistent. Therefore they may not be appropriate for use in further analysis.

2. MODEL DESCRIPTION

As implied in the *Bounding Calculations* portion of this report, there are two basic physical mechanisms that are believed to control the oil consumption due to vaporization from the ringpack – (1) oil vaporization and (2) oil vapor transport. Since the physical mechanisms that control the vaporization of liquid oil into oil vapor seem to be separate from the mechanisms that control the transport of the vapor from region to region, the modeling of the mechanisms are presented separately.

---

[2] Assuming oil is a single species of a purely paraffin hydrocarbon, the density of the saturated oil vapor at that

2.1. Oil Vapor Transport Model

"Oil Vapor Transport" is a phrase used here to describe the process by which oil vapor is carried from region to region within the ringpack. The view taken here is that oil vapor is simply carried along with the cylinder gasses as they blow into and out of the ringpack during the course of the engine cycle. Detailed knowledge of the gas flow through the different regions of the ringpack, therefore, is required in order to calculate oil vapor transport. Thankfully, the Ringpack-OC model already provides the needed data. Modeling oil vapor transport, therefore, will be a matter of defining how oil vapor is carried from region to region as determined by the Ringpack-OC gas flows.

2.1.1. Definition of Control Volumes

The modeling of any transport phenomenon requires the definition of control volumes upon which a mass balance can be applied. The control volumes (CV) used in this model will represent the various spaces between the piston, rings, and liner through which gasses can pass. A similar approach has been used by the Ringpack-OC model in its computation of the transport of cylinder gas through the ringpack. Because data is being fed from Ringpack-OC to this model, many of the control volumes used here are common to those used in Ringpack-OC (see Figure 28 below).

In both these models, individual control volumes are defined for the space between the piston crown land and the liner, the space between the second land and the liner, and the space between the third land and the liner. Also, the regions behind the top ring and behind the second ring are each given their own control volume. In addition to these control volumes, a CV is defined to represent the gas contained in the combustion chamber and another CV is defined to represent the gas in the crankcase.

Since some regions within the piston-ring-liner system will have very small volumes[3], it has been decided that these small regions will not have the ability to *accumulate* oil vapor. These regions still may have oil vapor pass through them and they may generate oil vapor, but no oil vapor can be accumulated. Two classes of control volumes, therefore, are used in this model -- the regions that cannot accumulate vapor are defined to be *passages* while regions that can accumulate oil vapor are defined to be *reservoirs*.

---

temperature will be approximately 33.5 g/m^3 as calculated from tabulated hydrocarbon data [6].

[3] Some control volumes are considered to be small as judged by the average volume flow rate of gas through a control volume versus the volume of the control volume itself.

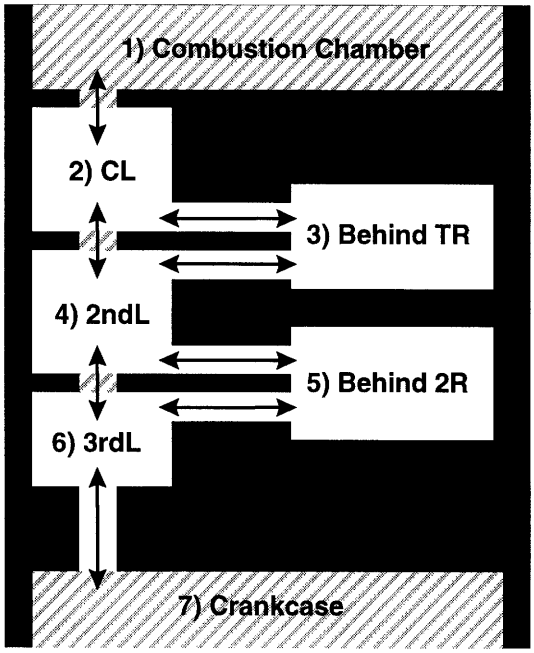

Figure 28: Control volumes used to model oil vapor transport through the system

Table 8: Definition of Regions In Model

Reservoirs	Passages
1) Combustion Chamber*	1) Comb Chamber to Crown Land*
2) Crown Land	2) Top of Top Ring Groove
3) Behind Top Ring	3) Top Ring Gap*
4) Second Land	4) Bottom of Top Ring Groove
5) Behind Second Ring	5) Top of Second Ring Groove
6) Third Land	6) Second Ring Gap
7) Crankcase*	7) Bottom of Second Ring Groove
	8) OC Ring/Piston Shirt/etc

*Note: No oil vapor generation (no oil vaporization) in these regions

With the control volumes defined, notice how there is a *network* of connections from control volume to control volume. This is not a linear map. Since the transport of oil vapor is determined by the overall gas flow from CV to CV, the gas flow between these regions must also be known. Making the control volumes here similar to those used in Ringpack-OC allows makes it possible to use the detailed gas flow output of Ringpack-OC. It is not necessary to calculate those flows separately.

2.1.2. Control Volume Mass Balance

As stated previously, the oil vapor transport in each region is governed by a mass balance. The mass balance can be expressed as

$$\text{Reservoirs:} \quad \frac{dMass}{dt} = \sum \dot{M}ass_{in} - \sum \dot{M}ass_{out} + \dot{M}ass_{gen} \tag{12}$$

$$\text{Passages:} \quad 0 = \sum \dot{M}ass_{in} - \sum \dot{M}ass_{out} + \dot{M}ass_{gen} \tag{13}$$

where $\dot{M}ass_{in}$ and $\dot{M}ass_{out}$ are the mass flow rates of oil vapor into and out of each reservoir or passage. The summations are included because there may be multiple flows into and out of each control volume. The $\dot{M}ass_{gen}$ term represents the total rate of oil vaporization in that particular reservoir or passage. Finally, the dMass/dt term represents the rate of oil vapor mass being accumulated in that particular reservoir.

In evaluating the above mass balances, it is necessary to know the causality – to know which terms are outputs of the equations and to know which terms are required inputs to the equations. For the reservoirs, it is necessary to know all the mass flow terms so that the accumulation term (dMass/dt) is the output. For the passages, there is no accumulation. An assumption is made, therefore, that information only flows downstream so that the inlet conditions are independent on what occurs within the CV. As a result, the $\dot{M}ass_{in}$ in an input along with the $\dot{M}ass_{gen}$ terms. The output term for the passages, is the vapor mass flow rate out of the CV, $\dot{M}ass_{out}$.

Since the oil vapor is being carried by the overall gas flow through the ringpack, computing the $\dot{M}ass_{out}$ term for the reservoirs is relatively straightforward. For each reservoir, for example, the value for $\dot{M}ass_{out}$ is found from

$$\dot{M}ass_{out} = \frac{Mass_{reservoir}}{Volume_{reservoir}} * \dot{M}_{gas\ flow} \tag{14}$$

where $Mass_{reservoir}$ is the mass of oil vapor in the reservoir and $\dot{M}_{gas\ flow}$ is the mass flow rate of gas leaving the reservoir. This value is obtained from the output of RINGPACK-OC. $Volume_{reservoir}$ is the open volume of the reservoir. This equation is used for each connection where gas is leaving a reservoir.

Since each reservoir is connected to a passage, the $\dot{M}ass_{in}$ for the connecting passage is the same value as the $\dot{M}ass_{out}$ term from the source reservoir. Similarly, once the $\dot{M}ass_{out}$ term is calculated for the passages, the $\dot{M}ass_{in}$ terms for the destination reservoirs are known.

The remaining quantities that need to be evaluated are the $\dot{M}ass_{gen}$ terms for both the passages and the reservoirs. These terms are found from the oil vaporization model...

2.2. Oil Vaporization Model

The basic assumption of the oil vaporization model is that every surface in the ringpack is wet with liquid oil and that the liquid oil generates oil vapor. As gas blows through the ringpack, it passes over the liquid oil and convects away the oil vapor being generated at its surface. The rate of convection is limited by the local momentum and mass diffusive properties of the gas boundary layer. In light of this view, the generation of oil vapor is modeled using a standard mass convection analysis.

Generally, mass convection is analyzed using an analogy between heat and mass transfer. In its simplest form, therefore, a mass transfer rate due to convection can be computed as [7]:

$$\dot{M}ass_{gen} = \overline{h_m} A_s (\rho_s - \rho_\infty) \tag{15}$$

where $\overline{h_m}$ is the average mass convection coefficient, A_s is the surface area generating vapor, ρ_s is the density of the vapor at that surface (saturation density), and ρ_∞ is the vapor density in the free stream. Notice that the amount of vapor convected is proportional to the difference between the vapor density at the surface and the vapor density in the free-stream. This is the relation used to calculate the rate of oil vaporization from the reservoirs.

In the passages, however, the gases will be flowing through small, enclosed pathways (internal flow). As the gas passes through the passages, the free-stream gas quickly gathers vapor. Equation (15) would still apply but, in implementing a numerical solution, a fine spatial grid and a small integration step would be needed in order to capture the quickly changing free stream vapor density as the gas moved through the passage. The reservoirs, having a much larger amount of free-stream gas to dilute the newly generated vapor, do not have this problem.

To avoid this expensive numerical implementation for the passages, the following internal flow relation is used to calculate the outlet vapor density given the inlet vapor density and a constant surface vapor density (ref. [7], equation 8.42b modified for mass transfer):

$$\frac{\rho_s - \rho_{out}}{\rho_s - \rho_{in}} = \exp\left(-\frac{A_s}{Q_{gas}} \overline{h}_m \right) \tag{16}$$

In this expression, $\bar{h}_m$ is the average mass convection coefficient for the region and Q_{gas} is the volumetric flow rate of gas through the region. The total vapor mass generated for a particular passage can then be found from:

$$\dot{Mass}_{gen} = Q_{gas}(\rho_{out} - \rho_{in}) \tag{17}$$

Note that the above formulations for calculating oil vapor generation do allow for oil vapor to be convected back toward the surface thereby removing oil vapor from the gas stream. Therefore, while no explicit modeling of vapor condensation is included, this formulation does allow for vapor to return to the surface if the gas flow becomes super-saturated (which might happen if the gas passes from a hot region of the ringpack into a cool region).

As with any convection problem, the difficult part of the analysis is in calculating an appropriate value for the convection coefficient, $\bar{h}_m$. Because of the analogy between heat and mass transfer, correlations developed for heat convection can be used for mass convection by substituting the appropriate dimensionless quantities. The substitutions are shown below:

Table 9: Definition of dimensionless terms in analogy between heat and mass transfer analysis

Heat Transfer		Mass Transfer	
Nusselt Number, *Nu*	$\frac{hL}{k}$	Sherwood Number, *Sh*	$\frac{h_m L}{D_{ab}}$
Prandtl Number, *Pr*	$\frac{\upsilon}{k}$	Schmidt Number, *Sc*	$\frac{\upsilon}{D_{ab}}$

In these expressions, L is a characteristic length, D_{ab} is the binary gas diffusion coefficient, ν is the kinematic viscosity of the bulk gas, and k is the thermal diffusivity of the bulk gas. In evaluating the quantities for this system, L is taken to be the hydraulic diameter for the given region, D_{ab} is the diffusion coefficient of oil vapor in air, and ν is the kinematic viscosity of the gas flow (air).

Solving for the convection coefficient requires a correlation based on the flow regime and fluid properties. In this model, two different internal flow correlations are used – one for laminar flow and one for turbulent flow. For this model, the transition between laminar and turbulent flow is assumed to take place at a Reynolds number of 4000.

For laminar flow with a combined thermal/velocity entry length, equation 8.57 from Incropera & DeWitt [7] is used:

$$\overline{Sh}_D = \left(\frac{7.54}{3.66}\right) 1.86 \left(\frac{\mathrm{Re}_{Dh}\, Sc}{4D_h}\right)^{\frac{1}{3}} \left(\frac{\mu}{\mu_s}\right)^{0.14} \tag{18}$$

The first coefficient (7.54/3.66) adjusts the correlation for flow between flat plates (the assumed geometry for these regions). Also, the viscosity ratio (μ/μ_s) is always equal to 1.0 because it is assumed that the free-stream viscosity does not differ from the viscosity near the surfaces simply due to differing concentrations of oil vapor.

For turbulent flow, only the relations for fully developed conditions are readily available. Equation 8.60 from Incropera & DeWitt [7] is used:

$$\overline{Sh}_{Dh} = 0.023 \mathrm{Re}_{Dh}^{4/5}\, Sc^{0.4} \tag{19}$$

With the average Sherwood numbers known, the convection coefficient can be found through the relation in Table 9. The convection coefficient is then used with the equilibrium surface vapor density in equations (16) and (17) to compute the total mass convection rate for the passages or in equation (15) to compute the total mass convection rate for the reservoirs. Once the convection coefficients are known, then the mass balances (equations (12) and (13)) can be evaluated for each region. The equations for the passages can be evaluated for $Mass_{out}$ and the equations for the reservoirs can be evaluated for d*Mass*/d*t*. Given initial conditions, this derivative can be integrated through time and the problem solved.

2.3. Evaluating Properties

While all the terms are solved for, it is still necessary to evaluate the expressions using actual numbers. To do this, several thermo-physical properties of the liquid oil, oil vapor, and ringpack gasses must be known for the various temperatures and pressures encountered in an internal combustion engine.

2.3.1. Oil Model

Evaluating the properties of engine oil is not always a trivial task. Engine oil is a complex mixture containing a range of heavy hydrocarbons species as well as any performance enhancing additives added by the manufacturer. Certain simplifications must be made in order to make the computations and modeling simpler.

As a first approximation, it is assumed that the engine oil is made of a single species of purely paraffinic hydrocarbon. The benefits of this model are that the properties of paraffinic hydrocarbons are tabulated and easy to find for a wide range of molecular weights. Also, all of the uncommon thermo-physical properties necessary to use this model can be found simply by defining the boiling point or the molecular weight for the hydrocarbon being used to model the engine oil. More common properties (such as density) must be specified by the user or by representative values for generic engine oil.

For the details of calculating the hydrocarbon's properties based on its boiling point, refer to Appendix A.

2.3.2. Gas Model

Like the engine oil, the gasses flowing through the ringpack are sure to have a complex composition. While most of the gas is sure to be air, it is likely to be mixed with liquid and vaporized fuel, liquid and vaporized engine oil, and combustion products. To compute the properties of this mixture, the first approximation is taken again – it is assumed that the properties are close to that for air at the same temperature and pressure.

2.3.3. Temperature Model

As seen in the *Estimating Oil Vaporization From The Cylinder Liner* portion of this report, temperature is an important parameter in vaporization calculations. In this model, it is necessary to specify the temperature of piston at several locations (land temperatures, ring groove temperatures, etc). The locations of the temperature definitions are the same as used in the Ringpack-OC model. At any location where such a definition does not directly apply, the local temperature is interpolated based on known temperatures that are nearby.

For the oil in the top of the top ring groove, for example, two different surfaces are exposed to the gas flow – (1) the top of the top ring groove and (2) the top of the piston ring. The temperature of the oil in this control volume is assumed to be the average of the temperature of these two surfaces. The temperature of the top of the top ring groove is defined to be the average of the crown land temperature and the temperature at the back of the top ring groove. The temperature of the top of the piston ring is assumed to be equal to the temperature of the piston ring itself. The piston ring, for lack of a better value, is assumed to be equal to the temperature of the back of the top groove. The temperature of the oil in the top of the top ring groove, $OilTemp_{TTRG}$, therefore, is calculated to be

$$OilTemp_{TTRG} = \frac{\left(T_{TTRG} + T_{ring}\right)}{2} = \frac{1}{2}\left(\left(\frac{T_{BTRG} + T_{CrwonLand}}{2}\right) + \left(T_{BTRG}\right)\right) = \frac{3}{4}T_{BTRG} + \frac{1}{4}T_{CrownLand} \quad (20)$$

where the T is the temperature, the subscript *TTRG* is the top of the top ring groove, and the subscript *BTRG* is the back of the top ring groove. The other groove temperatures are computed similarly.

Given the temperatures of the piston and liner (as discussed above), the local oil temperature and the local gas temperature is assumed to be the same as the local piston or liner temperature. For the passages, however, it is assumed that the gas enters the passage at the temperature of the source reservoir and exits the passage at the temperature of the passage itself (as calculated above). The mean temperature for the gas in the passage, therefore, is the average of the temperature of the source reservoir and the local passage temperature. These temperature values, as well as the dependent thermo-physical properties, are computed at each time step based on the source of the flow through a given passage.

Currently, no *physics*-based thermal model for a dynamic oil film temperature or gas temperature is included. Only the rules and assumptions presented here for the temperatures of the various bodies and fluids are used.

2.3.4. Pressure Model

Ringpack-OC computes the gas pressure for several regions within the ringpack. Those pressures are used directly where applicable. In the connecting passages between the reservoirs (between the regions where Ringpack-OC gives the pressure), the average pressure between the two connecting reservoirs is used. No physics-based modeling is used to try and improve this average pressure estimate.

2.4. Model Implementation

With all the geometry and physics defined, specific engines can be simulated by applying the model and equations described in the previous sections. The equations ultimately lead to several time-derivatives (equation (12)), one for each reservoir, which must be integrated through time in order to find the steady-state behavior of the system.

In the implementation presented here, these equations are integrated using a simple Euler numerical integration scheme. The time-step, however, is variable. The time step will shrink if the amount of oil vapor within any reservoir will change more than a given percentage based on the

current time step. For example, if the amount of oil vapor in the top land is going to decrease by 5% during the current time step, then the time step will be halved several times until the decrease becomes less than 1% in the current time step. Alternatively, the time step will increase if the change in oil vapor in every reservoir is greater than 0.1% per time step. The specific thresholds for these changes are user-definable.

Finally, since it is the steady-state oil vaporization that is of interest to the user, it is necessary to (1) specify the initial amount of oil vapor in each reservoir, (2) run the simulation, and then (3) check to see if the model returns back to those initial values at the end of the cycle. If the beginning and ending values do not match, then new initial values must be chosen and the simulation run again. In later incarnations of the model implementations, this process has been automated such that the user must simply allow the model to run several cycles so that the proper initial states and steady-state behavior are found iteratively.

2.5. Model Summary

This section of this report presents a model that estimates the amount of oil vaporization from various regions within the piston-ringpack-liner system. One application of this model is to compute the amount of oil consumed by the engine due to vaporization from the piston-ringpack-liner region.

The model is composed of two main parts: (1) a mass transport model and (2) a mass convection model.

The mass transport model calculates how oil vapor moves from one region of the ringpack to another based on the instantaneous motion of cylinder gasses blowing through the ringpack. As a result, it also computes how much oil vapor is carried back into the combustion chamber which, as is assumed here, gives the desired value for oil consumption due to vaporization from the ringpack.

The mass convection model computes how much oil vapor is generated by the gasses in the ringpack as the flow over the liquid oil within the ringpack. The mass convection model is based on the analogy between heat and mass transfer for internal flow situations.

In evaluating the equations used in the model, it is necessary to know several thermo-physical properties of the liquid oil, the oil vapor, and the ringpack gasses. The properties of the liquid oil and oil vapor are found by assuming the oil is composed of a single species of paraffin hydrocarbon. Given the user-defined boiling point of this hydrocarbon, most of the necessary properties are

computed within the model. The properties for the ringpack gasses are assumed to be the same as those for air at the same temperature and pressure.

2.6. Summary of Assumptions

Listed below are many of the assumptions that are part of the current model or its implementation. These assumptions represent the most important points to keep in mind when the results generated by the model. Also, this list represents the best place to begin when looking for ways to improve the model. Many of these assumptions were made because they would greatly decrease the time needed to develop the model. They may not have been chosen because they were the best way to physically model the system.

2.6.1. General Assumptions

1. Any vapor reaching combustion chamber is lost from the system (this is the quantity defined as the amount of oil consumed due to vaporization from the ringpack)
2. Any vapor reaching crankcase is lost from the system (not included as consumption)
3. Vapor density of any gas flowing from the crankcase is assumed to be zero
4. No vapor is generated by gas flowing through the ring gaps

2.6.2. Temperature Assumptions

1. All temperatures remain constant in time
2. The gas flow through each region assumes the temperature of the surface of that region
3. The surface temperatures of reservoirs are defined from RINGPACK-OC input
4. The surface temperatures of the passages are defined by the average of the temperatures of the connected reservoirs
5. The temperature of the gas in the lands is the average of the liner temperature and the temperature of the land
6. The liner temperature is constant along its length

2.6.3. Geometry Assumptions

1. All regions are modeled as regular rectangular prisms
2. The rings are fixed in the center of the groove
3. The volume of the regions around the rings is reduced by the amount of resident oil as defined in the RINGPACK-OC input
4. All surfaces stay fully wetted with oil regardless of the rate of oil vaporization

2.6.4. Oil Assumptions

1. Single species (boiling point given as input)
2. Purely paraffin hydrocarbon

2.6.5. Numerical Implementation

1. Simple Euler integration scheme used to integrate through time the changing oil vapor in each reservoir.
2. Variable time step that will change if the mass in any reservoir changes more than a certain user-defined percentage of its current amount (typically 0.1%-1%).

3. RESULTS AND DISCUSSION

3.1. Description of Engine and of Baseline Case

To generate the results presented in this section, the same Cummins diesel engine is simulated as in prior sections (table 1and table 3). Also the same 2200 RPM, full load baseline operating condition used in the previous sections was used as the baseline case for this study (table 2). Being a vaporization model, it is necessary to specify the local temperature of several regions within the piston-liner-ringpack system. At the baseline operating condition, the values in table 10 are used.

Table 10: Temperatures for various regions of the system as used for simulations at the baseline operating condition.

Average liner temp	125 C
Temperature of top land	355 C
Temperature behind top ring	296 C
Temperature of second land	238 C
Temperature behind second ring	233 C
Temperature of third land	228 C
Temperature of crankcase	150 C

The oil used in the simulations is the same Cummins Premium Blue SAE 15W40 oil used in previous studies of this report. Since this oil vaporization model only accepts the input of a single boiling point for the oil, however, any distinguishing behavior of the Cummins 15W40 from any other SAE 15W40 will be difficult to see. As a first approximation, the boiling point for the Cummins SAE 15W40 oil is taken to be the temperature from the distillation curve when 50% of the oil has vaporized. Referring back to figure 3, this value is seen to be approximately 715K.

Complicating the issue of choosing an appropriate boiling point, it was seen in the results from the LinerOilVap model that oil composition could change due to oil vaporization. In locations where oil supply is limited, the vaporization depletes the local oil of its more volatile species. The oil's average boiling point was seen to increase. Looking back to figure 14, the mean boiling point was seen to vary from the normal 715K to an upper value of 738K. Without a detailed oil transport model for the movement of liquid oil within the ringpack, the oil supply to the various surfaces in the ringpack is unknown. The local oil composition cannot be predicted without this information. Therefore, it is necessary to assume a mean boiling point for the oil in the ringpack.

In the ringpack, with its much hotter local temperatures, the range of oil composition could be much larger than the 23K range seen for the oil on the liner. The uncertainty of the oil's composition is much larger in the ringpack. As a result, simulations will be performed using a wide range of mean oil boiling points (715K through 835K). Since the model does not allow for local variations in oil composition, the specified boiling point applies to all oil within the ringpack and on the liner.

Detailed geometry and operating conditions as well as a cylinder pressure trace for this engine are used to run the ring and gas dynamics model, Ringpack-OC. Some results from Ringpack-OC are presented in figures 29-31 below.

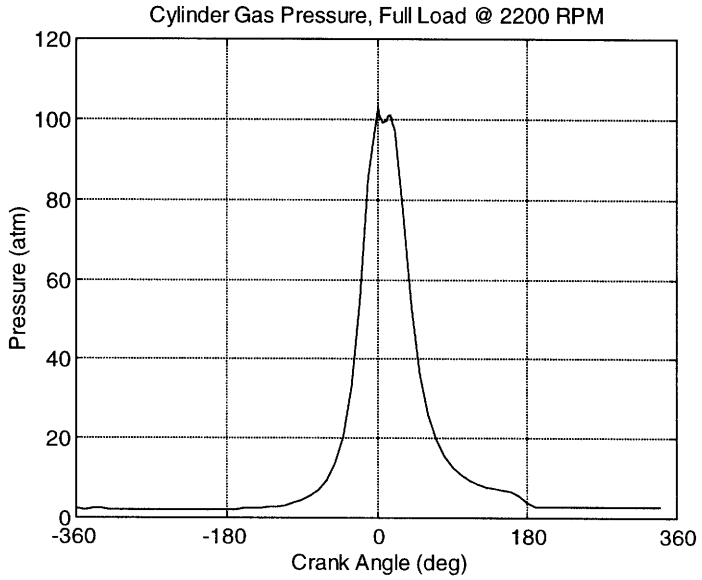

Figure 29: Estimated cyclic variation of the pressure of the cylinder gasses at full load and 2200 RPM

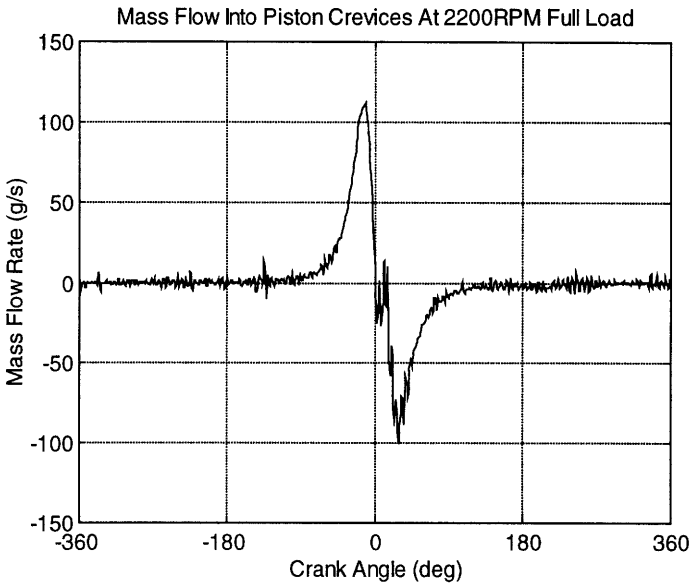

Figure 30: Mass flow rate of gas into piston crevices from cylinder at 2200 RPM and full load

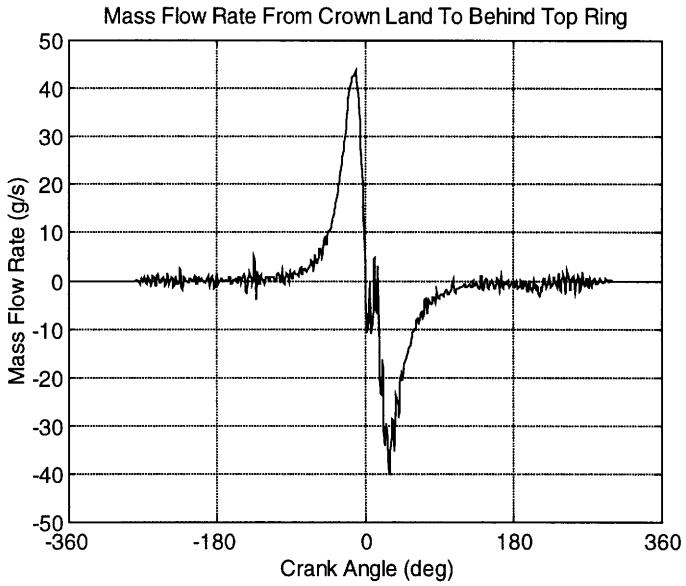

Figure 31 A: Estimated mass flow rate of gas at 2200 RPM and full load from (A) crown land to region behind top ring

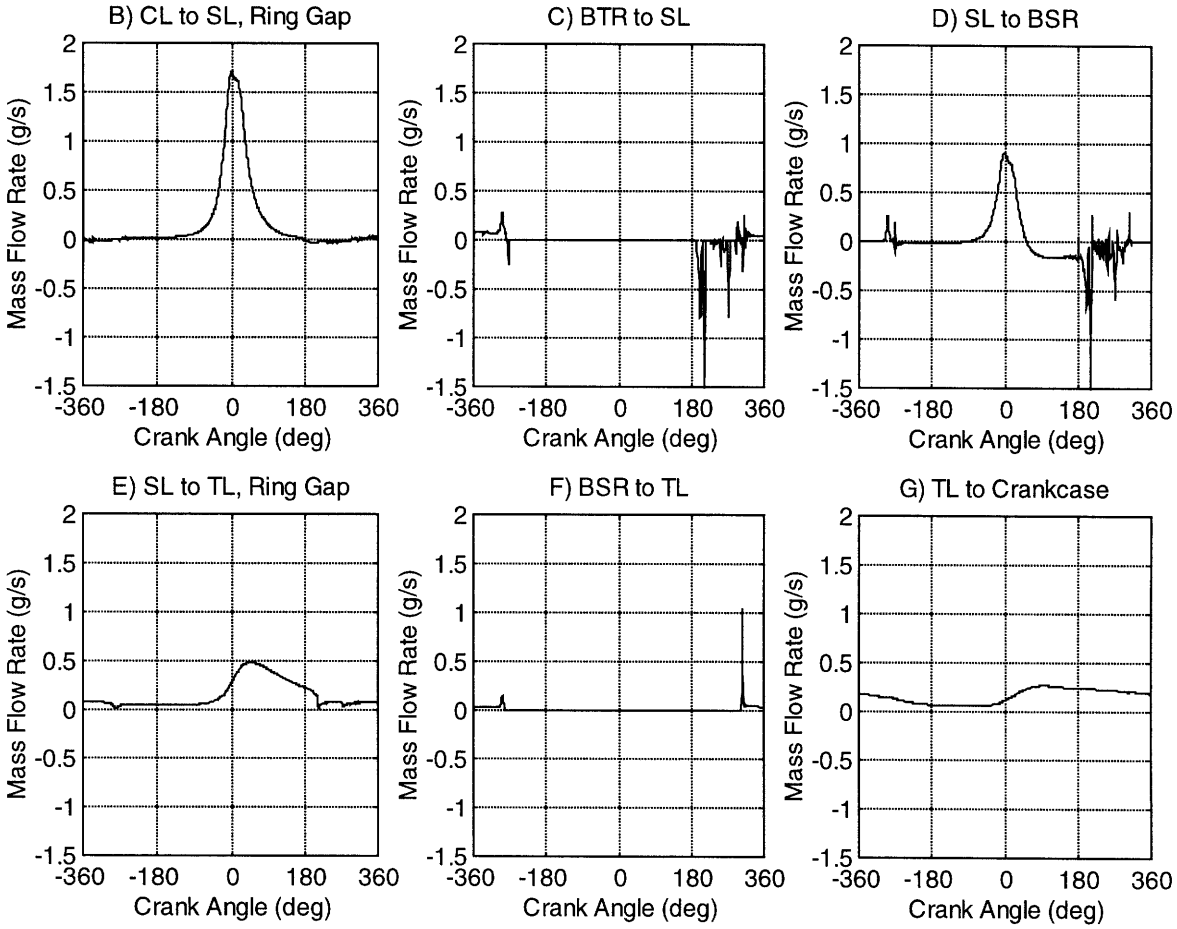

Figure 31 B-G: Estimated mass flow rate of gas at 2200 RPM and full load from: (B) crown land to second land through ring gap, (C) behind top ring to second land, (D) second land to behind second ring, (E) second land to third land through the ring gap, (F) behind second land to third land, (G) third land to crankcase.

Comparing figures 29 and 30, notice that gas flows into the ringpack as the cylinder pressure increases during the compression stroke (-180 deg CA through 0 deg CA). Then, as the cylinder pressure decreases during the expansion stroke, the flow reverses direction and gas blows out of the ringpack back into the cylinder. It is this reverse blow-by that will carry the oil vapor out of the ringpack and into the combustion chamber.

Figures 31 A-G show how and when gas moves between the various regions within the ringpack. These gas flows control how oil vapor will be transported between the regions as well as how much vapor is generated through convection.

As an interesting side comment, notice the highly variable flow in figures 31C and 31D during the exhaust stroke (the spiking behavior). This behavior is caused by the top ring losing its seal against the bottom of the top ring groove. While in this vaporization model, the ring is assumed

to be fixed in its groove, the ring and gas dynamics model allows the ring to move. When the ring looses its seal, the opposing gas pressure and ring inertia forces cause the ring to flutter. The fluttering allowing gases to burst through intermittently as the ring waivers between its sealed and unsealed positions within the groove.

3.2. Quantifying Vaporization Rates

After running the model for several cycles, the steady-state rate of oil transport to the combustion chamber due to vaporization from the ringpack can be found. This transport rate can be considered the rate of oil consumption due to oil vaporization from the ringpack. The results are presented in table 11 below.

Table 11: Rate of oil consumption due to oil vaporization from ringpack for 2200 RPM, full load.

Average Oil Boiling Point Used in the Simulation	Rate of Oil Consumption Due to Vaporization From the Ringpack
715 K	27.22 g/hr/cylinder
775 K	3.609 g/hr/cylinder
835 K	0.3574 g/hr/cylinder

Compared with the total oil consumption value of 10-13 g/hr/cylinder expected from the actual engine, the baseline case (715 K) clearly over-estimates the oil vaporized from the ringpack. The other two values, however, are more reasonable. The wide spread of values in this table shows the strong dependence of oil vaporization on oil composition. It would be very helpful to have an oil transport model for the ringpack so that the oil supply to the surfaces in the ringpack could be known. Such information would be necessary to calculate the local oil composition in the various regions. Knowing the local oil composition would allow the model to calculate if the vaporization from the ring pack is closer to the 3.6 g/hr value (a significant contribution to overall oil consumption) or closer to the 0.36 g/hr value (an insignificant contribution to overall oil consumption).

Since the 3.6 g/hr value is a more reasonable estimate compared to the 27.22 g/hr, the remaining results are presented for the case using the oil with a boiling point of 775 K.

3.3. Timing of Vapor Transport To Combustion Chamber

Figure 32 shows the amount and the timing of the expulsion of oil vapor from the ringpack into the combustion chamber using the oil with boiling point of 775K.

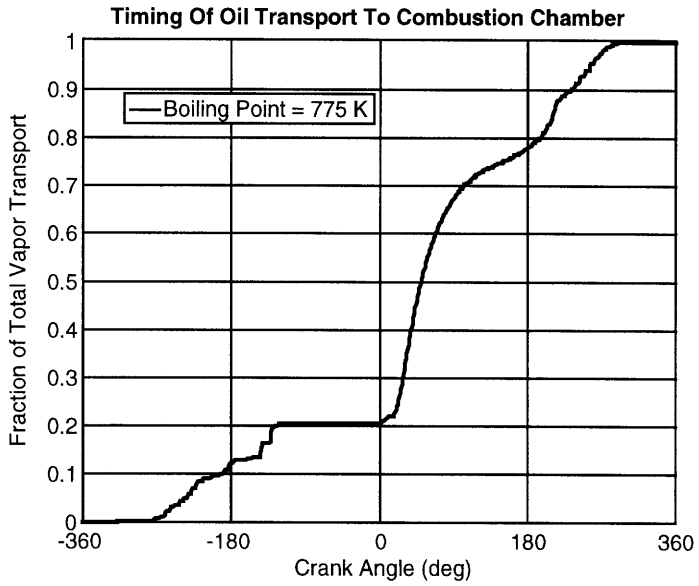

Figure 32: Timing of transport of oil vapor from the ringpack to the comubstion chamber for 2200 RPM, full load.

Note that most of the oil vapor is transported to the combustion chamber during the expansion stroke (57 % during 0 degrees through 180 degrees). This could have significant effect on the type of emissions generated by this engine (such as heavy hydrocarbons, partially burned hydrocarbons, or soot) because the timing of the arrival of the oil vapor to the combustion chamber affects how much of that vapor can be burned. For that portion of the vapor that reaches the combustion chamber late in the cycle, it may exit the engine completely unburned whereas vapor that reaches the combustion chamber prior to ignition may exit the engine completely burned.

3.4. Location of Vaporization

Figure 33 shows where vaporization occurs in the simulation of the system using the 775K boiling point oil. Positive values represent oil being vaporized while negative values represent oil vapor condensing back into liquid oil. The names of the various regions such as "R1" and "P3" represent names such as "Reservoir 1" and "Passage 3". The reservoir and passage numbering scheme is defined in table 8 in the *Model Description* section of this report.

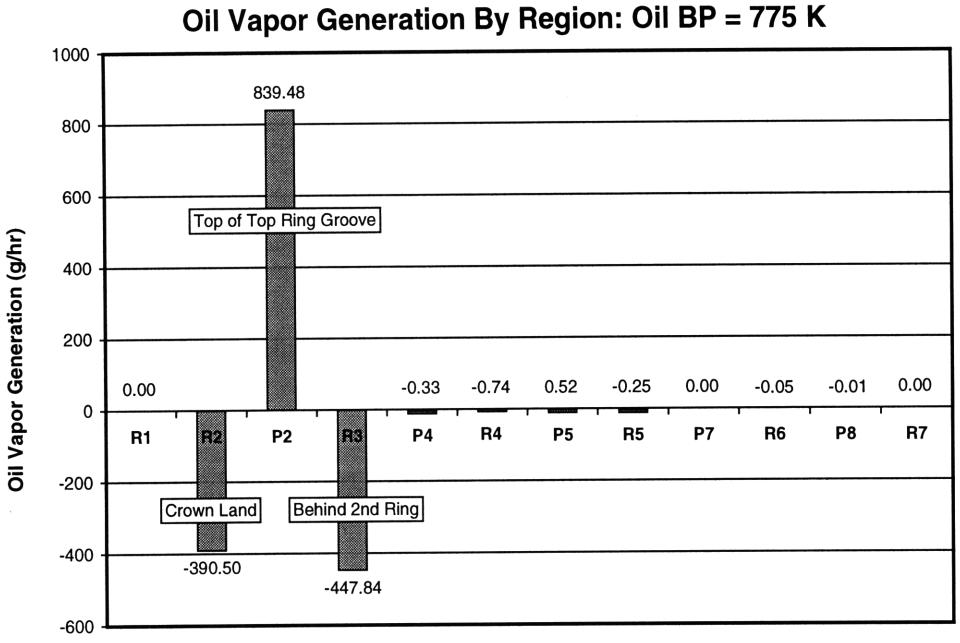

Figure 33: Oil vaporization by ringpack region at 2200 RPM, full load, and using an oil with a boiling point of 775 K.

Notice that a large amount of oil vaporization occurs in top portion of the top ring groove. Then, a significant portion of that oil is condensed in the adjoining reservoirs representing the crown land and the back of the top ring groove. This behavior could be explained by the fact that the temperature of the region behind the top ring is defined to be cooler than top of the top ring groove. Also, the temperature of the oil on the crown land (and liner next to the crown land) is defined to have a temperature equal to the average of the crown land and liner temperature. This average temperature will also be cooler than the temperature of the top of the top ring groove.

As seen in back in figure 31(A), the flow rate into the back of the top ring groove is the dominant flow in the system. Therefore, as gas flows into the system from the combustion chamber, most of the gas flows past the top of the top ring groove thereby gathering much oil vapor. When it reaches the back of the top ring groove, it sits there and accumulates waiting for the flow to reverse and exit back to the combustion chamber. As it sits in the cooler back-of-the-ring-groove region, much of the vaporized oil condenses. Once the flow reverses and beings travels from the back of the top ring groove, past the top of the top ring groove, and through the crown land region, this vaporization/condensation routine repeats again. In this flow regime, though, the oil vapor gained in from the top of the top ring groove is condensed onto the crown land and nearby liner.

3.5. Excessive Localized Vaporization

Looking back at the amount of oil vaporized from the top of the top ring groove, it appears that too much oil may be vaporizing from this one location. One of the assumptions of this model is that every surface stays wetted with liquid oil (there is an infinite supply of liquid oil) regardless of the vaporization rate. In reality, of course, this is not true. Too much vaporization could completely dry a given region of the ringpack of its oil. Therefore, it is necessary to see if the amount of oil vaporized from each region seems to be within appropriate bounds. For the top of the top ring groove, this may not be true.

By dividing the average vaporization rate from this region (840 g/hr) by the surface area of the region (2.2 cm^2), there is a net oil loss of 125 micron/sec. Given the long and circuitous route that liquid oil must take to get to this region of the piston, it seems unlikely that 840 g/hr of oil can be transported to replace this amount of vaporized oil (though not impossible knowing that the scraping rate by the second ring was reported in table 6 to be about 2000 g/hr). It appears, therefore, that the model's assumption of infinite liquid oil supply may be inadequate because the top of the top ring groove may, in fact, run out of liquid oil.

If the top of the top ring groove does vaporize all of the liquid oil available to it, then the results predicted by this model are incorrect. This model assumes that the vaporization of oil is limited by the ability of the gas flow to convect oil vapor from the wetted surfaces of the ringpack. In the case of the top of the top ring groove, it appears that the system may be limited by the supply of liquid oil to the system.

To correctly model the supply-limited case, additional physics must be added to the current model. Specifically, the mechanisms that control the transport of liquid oil through the system must be appropriately modeled. Such modifications are not performed here and should be added as part of some later study.

4. SUMMARY AND CONCLUSIONS

A model has been formulated to estimate the rate of oil consumption due to vaporization from the piston-ring-liner system. The model assumes that the rate of vaporization is limited by the rate at which the vapor can be convected away from the wetted surfaces within the system. Once convected away from the surfaces, the model computes how the vapor is transported throughout the system until

it eventually reaches the combustion chamber. Once it reaches the combustion chamber, the oil vapor is assumed to leave the engine and is considered to be consumed.

Being a convection-based model, the model requires detailed knowledge of gas flow through the ringpack. This information is obtained by using a separate ring and gas dynamics model, Ringpack-OC.

For a heavy-duty diesel engine running at 2200 RPM, full load and using a single-species model for an SAE 15W40 engine oil, the following results are found:

1. The rate of oil consumption due to oil vaporization from the ringpack was found to be 3.6 g/hr/cyl or 30% of the total expected for an engine in this class. This value is *highly* sensitive to local oil composition, which is an unknown parameter.
2. Most (57%) of the oil vapor reached the combustion chamber during the expansion stroke.
3. A large amount of vaporization (840 g/hr) was found to occur in the top portion of the top ring groove though most of that vapor was quickly condensed back to liquid in nearby regions within the ringpack.

Because the rate of vaporization from the top of the top ring groove is so high, it is very possible that this region could vaporize all the oil available to it. In such a situation, the model presented here does not correctly predict the behavior of the system. Improvements to the model must be made so that the supply of liquid oil to top of the top ring groove is properly calculated.

SUMMARY AND CONCLUSIONS

1. OVERVIEW

Two models have been developed to estimate in-cylinder sources of oil vaporization in internal combustion engines. One model estimates the rate of oil vaporization from the cylinder liner while the other model estimates the rate of oil vaporization from the surfaces in the piston ringpack and adjoining cylinder liner. The purpose of these models is to gauge the importance of oil vaporization relative to overall oil consumption in an internal combustion engine.

The models were physics-based and assumed that oil vaporization was a convection-driven process. For both models it was necessary to define a convection sub-model appropriate for the given gas flow and geometry. Both vaporization models also required sub-models to describe the behavior of the convecting gas and to describe the behavior and properties of the liquid oil. These tasks were handled by existing models external to the vaporization model or sub-models were created and included internal to the vaporization model.

Both models were implemented numerically. The two computer programs perform their analyses on a crank-angle by crank-angle basis and can provide detailed information as to what the model believes to be the internal state of the system being modeled. Being computer programs, the models can be easily used to perform parametric studies to see what design and operating parameters affect oil vaporization.

2. SUMMARY OF RESULTS

The models developed here were all used to examine the behavior of a Cummins heavy-duty diesel engine running at a baseline operating condition of 2200 RPM at full load while Cummins Premium Blue (SAE 15-W40) engine oil. By simulating this baseline case, and by varying parameters around this case, several results were found that:

For the liner oil vaporization model:

1. Vaporization from the liner is about 1.3 g/hr/cylinder, or, about 10% of the total oil consumption expected for this engine.
2. Vaporization is strongly dependent on liner temperature (order-of-magnitude ever 38 degrees), steady-state oil composition (66% increase using different but related oil), and the parameters used internally to model the mass convection (factor of 3 above and below reported values).
3. Vaporization from the liner seems to have little dependence on engine speed. The cause for this result was not explored.

For the coupled liner oil vaporization / Friction-OFT model:

1. Oil is carried to the upper liner by attaching and detaching itself to the ring faces depending upon the dynamics of ring load and lubrication state.
2. Oil supply to the upper liner due to carrying by the rings is about 9.6 g/hr, or, about 20 times the rate of oil vaporization from this area. Most of the up-carried oil is later carried down out of the upper liner by the rings but its effect on the steady-state oil composition is important.
3. Doubling the ring tension acts to reduce the oil supply to the upper liner by 26%, increase scraping by 53%, and decrease liner oil vaporization from the upper liner by 23%.

And for the ringpack oil vaporization model:

1. The rate of oil consumption due to oil vaporization from the ringpack is about 3.6 g/hr/cylinder (arbitrarily assuming a mean oil boiling point of 775K).
2. The consumption values are *highly* dependent upon the assumed oil boiling point Vaporization ranges up to 27 g/hr using the mean boiling point for fresh oil -- 715K.
3. A large amount of vaporization happens in the top of the top ring groove – so much so that the fundamental assumptions of the whole model is mostly likely broken.

3. CONCLUSIONS

The purpose of this study was to develop models that could establish if oil vaporization was significant relative to the overall engine oil consumption. At the baseline conditions, both models

predicted that vaporization is significant. In some cases, especially with a hot engine or with a volatile oil formulation, oil vaporization could be the dominant form of oil consumption.

Both models, though, were highly sensitive to one or more of the input parameters. For example, local oil composition is not well known experimentally in the regions of the engine being considered here. Therefore, assumptions were made or additional modeling performed to estimate the local oil composition. Especially for the vaporization from the ringpack, if the local oil composition were better known, confidence in the results of the vaporization model would be increased significantly.

For both models though, there can be little confidence in the results without some measure of experimental validation. Lots of information is generated by the vaporization models and any bit of that information could be compared to experimental results to help confirm individual pieces of the models and to help give confidence to the models as a whole.

Comparing to intuition and experience, though, this study seems to be successful in developing models that estimate the rate of oil vaporization due to in-cylinder sources. The models are able to include the effect of a wide range of engine design and operating conditions while remaining relatively easy to set-up and use. They can be used to answer important questions about the sources of oil consumption and how that consumption might be controlled.

4. FUTURE WORK

As discussed previously, there are several areas where future work in this area can be focussed:

1. Some measure of experimental confirmation should be performed for the liner oil vaporization model.
2. A liquid-oil transport model to track oil movement through the ringpack should be included with the ringpack oil vaporization model. Such a model is necessary to compute the steady-state oil composition within the ringpack.
3. Once a liquid-oil transport model is included, the ringpack oil vaporization model should be modified to include a multi-species model for the liquid oil and oil vapor.
4. Additional physical processes need to be considered in the liner oil vaporization model so that the effects of liner roughness on liner oil vaporization can be captured and explored.

5. ACKNOWLEDGEMENTS

This work was supported by the MIT Consortium on Lubrication in Internal Combustion Engines and a fellowship from Cummins Engine Company. Members of the Consortium include Dana Corp., MAHLE, Peugeot SA, Renault and Volvo. The authors would like to thank Dr. Dan Richardson at Cummins for supplying engine test data during the course of model development. William Audette's education was supported by the Cummins Fellowship.

SUPPORTING MATERIAL

REFERENCES

1.1. Introduction

[1] Orrin, D. S. and Coles, B. W., (1971), "Effect of Engine Oil Composition on Oil Consumption", SAE Paper No. 710141

[2] Furuhama, S., Hiruma, M. and Yoshida, H., (1981), "An Increase of Engine oil Consumption at High Temperature of Piston and Cylinder", SAE Paper No. 810976

[3] Tian, T., Noordzij, L., Wong, V. and Heywood, J., (1996) "Modeling Piston-Ring Dynamics, Blowby, and Ring-Twist Effects", ICE-Vol. 27-2, 1996 Fall Technical Conference, Volume 2. ASME

[4] Tian, T., Wong, V. and Heywood, J., (1996), "A Piston Ring-Pack Film Thickness and Friction Model for Multigrade Oils and Rough Surfaces", SAE Paper No. 962032

1.2. Estimating Vaporization From The Cylinder Liner

[1] Orrin, D. S. and Coles, B. W., (1971), "Effect of Engine Oil Composition on Oil Consumption", SAE Paper No. 710141

[2] Furuhama, S., Hiruma, M. and Yoshida, H., (1981), "An Increase of Engine oil Consumption at High Temperature of Piston and Cylinder", SAE Paper No. 810976

[3] Wahiduzzaman, S., Deribar, R. and Dursunkaya, Z., (1992), "A Model for Evaporative Consumption of Lubricating Oil in Reciprocating Engines", SAE Paper No. 922202

[4] De Petris, C., Gigilio, V. and Police, G. (1997), "A mathematical Model of the Evaporation of the Oil Film Deposed on the Cylinder Surface of IC Engines", SAE Paper No. 972920

[5] Incropera, F. and DeWitt, D., (1990), *Fundamentals Of Heat Transfer*, Third Edition, John Wiley & Sons, New York, NY

[6] Assanis, D.N. and Heywood, J.B., (1986), "Development and use of Computer Simulation of the Turbocompounded Diesel System for Engine Performance and Components Heat Transfer Studies", SAE Paper No. 860329

[7] Lyman, W., Reehl, W. and Rosenblatt, D., (1990) *Handbook of Chemical Property Estimation Methods*. American Chemical Society, Washington, DC

[8] Froelund, K., Schramm, J., Tian, T., Wong, V. and Hochgreb, S., (1996), "Analysis of the Piston Ring/Liner Oil Film Development During Warm-Up for an SI-Engine", ICE-Vol. 27-2, 1996 Fall Technical Conference, Volume 2, ASME

[9] Tian, T., Wong, V. and Heywood, J., (1996), "A Piston Ring-Pack Film Thickness and Friction Model for Multigrade Oils and Rough Surfaces", SAE Paper No. 962032

[10] Tian, T., Noordzij, L., Wong, V. and Heywood, J., (1996) "Modeling Piston-Ring Dynamics, Blowby, and Ring-Twist Effects", ICE-Vol. 27-2, 1996 Fall Technical Conference, Volume 2. ASME

1.3. Oil Transport Along The Liner - Coupling Liner Oil Vaporization to Friction-OFT

[1] Tian, T., Wong, V. and Heywood, J., (1996), "A Piston Ring-Pack Film Thickness and Friction Model for Multigrade Oils and Rough Surfaces", SAE Paper No. 962032

1.4. Estimating Oil Vaporization From The Ringpack

[1] Wahiduzzaman, S., Deribar, R. and Dursunkaya, Z., (1992), "A Model for Evaporative Consumption of Lubricating Oil in Reciprocating Engines", SAE Paper No. 922202

[2] De Petris, C., Gigilio, V. and Police, G. (1997), "A mathematical Model of the Evaporation of the Oil Film Deposed on the Cylinder Surface of IC Engines", SAE Paper No. 972920

[3] Audette III, W., Wong, V., (1999), "A Model for Estimating oil Vaporization from the Cylinder Liner as a Contributing Mechanism to Oil Consumption", SAE Paper No. 1999-01-1520

[4] Tian, T., Noordzij, L., Wong, V. and Heywood, J., (1996) "Modeling Piston-Ring Dynamics, Blowby, and Ring-Twist Effects", ICE-Vol. 27-2, 1996 Fall Technical Conference, Volume 2. ASME

[5] Burnett, P., Bull, B., Wetton, R., "Characterisation of the Ring Pack Lubricant and Its Environment", Shell Research, Thorton Centre

[6] Wilhoit, R. C. and Zwolinski, B.J., (1971) *Handbook of Vapor Pressures and Heats of Vaporization of Hydrocarbons and Related Compounds.* Thermodynamics Research Center, Texas A&M University, College Station, TX

[7] Incropera, F. and DeWitt, D., (1990), *Fundamentals Of Heat Transfer*, Third Edition, John Wiley & Sons, New York, NY

1.5. Appendices

[1] Wilhoit, R. C. and Zwolinski, B.J., (1971) *Handbook of Vapor Pressures and Heats of Vaporization of Hydrocarbons and Related Compounds.* Thermodynamics Research Center, Texas A&M University, College Station, TX

[2] Gallant, R.W. and Yaws, C.L., (1993) *Physical Properties of Hydrocarbons and Other Chemicals.* Gulf Publishing Company, Houston, TX

APPENDIX A: CALCULATING OIL PROPERTIES

The first task necessary to compute the oil properties required by this model is to translate the data given by an oil distillation curve into useful information regarding the properties of the various species that compose engine lubricating oil.

As a modeling assumption, let all the components in engine oil be pure paraffin hydrocarbons. Using tabulated information from Wilhoit and Zwolinski [11],the molecular weight of such hydrocarbons can be reasonably correlated to the hydrocarbon's boiling point through

$$MW = (6.28x10^{-6}) \cdot T_{bp}^3 + (-4.61x10^{-3}) \cdot T_{bp}^2 + (1.953) \cdot T_{bp} - 99.93 \tag{A.1}$$

where MW is the specie's molecular weight (kg/kmol) and T_{bp} is the specie's boiling point (C) as reported from the distillation curve. This correlation is fitted to tabulated data over a temperature range of 460K through 900K.

Once the molecular weight is known, all the other necessary thermo-physical properties can be calculated because, for a pure paraffin hydrocarbon, the chemical structure is completely defined once the molecular weight is known. Since paraffin hydrocarbons have no branches, the chemical shape is that of a long string and the number of hydrogen atoms is exactly 12 times the number of carbon atoms plus 2 more to terminate both ends of the chain.

The vapor pressure can be computed knowing the chemical composition and the local instantaneous temperature of the liquid oil [1]

$$\log_{10}(VP) = A - \frac{B}{C + (T_l - 273)} \tag{A.2}$$

where VP is the vapor pressure (mm Hg), T_l is the temperature of the liquid at its exposed surface (Kelvin), and A, B, and C are the Antoine constants which are tabulated by oil species [1]. Assuming a paraffin structure, the constants are correlated to the oil specie's molecular weight through

$$\begin{aligned} A &= (4.40x10^{-10}) \cdot MW^3 + (-1.10x10^{-6}) \cdot MW^2 + (1.04x10^{-3}) \cdot MW - 6.85 \\ B &= (1.91x10^{-6}) \cdot MW^3 + (-4.78x10^{-3}) \cdot MW^2 + (4.51) \cdot MW - 1.06x10^3 \\ C &= (-1.15x10^{-7}) \cdot MW^3 + (4.03x10^{-4}) \cdot MW^2 + (-6.02x10^{-1}) \cdot MW - 2.72x10^2 \end{aligned} \tag{A.3}$$

As before, these correlations are fitted to tabulated data. The source data was taken over the *MW* range of 310 kg/kmol to 842 kg/kmol.

Note that equation (A.2) becomes unbounded the sum ($C+T_l$) approaches zero. In order a species in the liner oil to reach this temperature, however, the vapor pressure will have passed the point where it exceeds the total pressure within the cylinder. When this happens, the species will boil and the resulting the mass transfer is no longer diffusion limited (as this model assumes) but is, instead, energy limited. The physics of the boiling process are not included in the current model. In the results shown in this report, however, the temperature of the liquid oil was never high enough to cause any species to boil.

In addition to the oil properties, the thermo-physical gas properties necessary to calculate vaporization are calculated using thermodynamic tables for air. In all cases, both the instantaneous cylinder pressure and the instantaneous boundary layer film temperature are used for evaluating the gas properties. Due to the low mass fraction of the oil vapor in the air, this should be a reasonably valid assumption.

The binary diffusion constant of a given oil species through air was computed using an algorithm presented in [2].

APPENDIX B: DERIVATION OF EXPRESSION OF MASS CONSERVATION UNDER RING FACE

In order to find the steady-state composition of the oil on the cylinder liner, it is necessary to know both how the oil is removed from the liner (vaporization) and how oil is supplied to the liner (ring motion). On a volume basis, it is known how the oil is supplied to the liner -- the liner oil film thickness model by Tian et al. (1996) gives this information. It is still necessary, however, to compute how the *composition* of the oil changes by the passage of the rings.

Using the modeling assumptions laid out in the Description of Model section of this report, it is assumed that oil attached to the face of the ring as it moves up and down the liner. A control volume can be drawn about this region and a conservation of mass can be applied

$$\frac{d}{dt}\left(mass_{stored}\right) = \dot{mass}_{in} - \dot{mass}_{out} \tag{B.1}$$

Since the movement of oil in terms of volume is known, it is easier to track simply the composition of the oil. Rewriting the equation in terms of the mass fraction of each species *i*, the conservation of mass becomes

$$\frac{d}{dt}\left(mf_{stored,i} \cdot Vol_{stored}\right) = \left(mf_{in,i} \cdot \dot{Vol}_{in}\right) - \left(mf_{out,i} \cdot \dot{Vol}_{out}\right) \tag{B.2}$$

Finally, rewriting the volume flow rate terms in the variables described back in figure 5 as well as in terms of the piston velocity, *Vel*, and the cylinder radius, *R*, the conservation of mass on the control volume is

$$\frac{d}{dt}\left(mf_{stored,i} \cdot Vol_{stored}\right) = Vel \cdot 2\pi \cdot R \cdot \left(\left(h_{in} \cdot mf_{in,i}\right) - \left(h_{out} \cdot mf_{out,i}\right)\right) \tag{B.3}$$

When carrying out the time integration of these *i* equations, it is necessary to remember that the sum of the mass fractions is supposed to exactly equal one. Using normal numerical integrator routines (Euler, Runge-Kutta, etc), the sum of the mass fractions will deviate from one. It is necessary to renormalize the values of the mass fractions so that they sum to a value of one at every time step.